EVALUATION OF ALTERNATIVE COOLING TECHNIQUES

FOR PHOTOVOLTAIC PANELS

by

HAMIDREZA NAJAFI

KEITH A WOODBURY, COMMITTEE CHAIR

JOHN BAKER
MUHAMMAD ALI ROB SHARIF

A THESIS

Submitted in partial fulfillment of the requirements
for the degree of Master of Science
in the Department of Mechanical Engineering
in the Graduate School of
The University of Alabama

TUSCALOOSA, ALABAMA

2012

ABSTRACT

The growing worldwide demand for electricity, rising fossil fuels prices and increasing concerns about global warming, have renewed attention in renewable energies during last decades. Solar energy is the most abundant source of energy on the earth. Although technologies for converting sunlight energy to power have made a lot of progress, high capital cost and low conversion efficiency are the main hurdles for widespread use of these technologies. Using different methods in order to increase the efficiency of solar power generation and make it a more cost effective technology have been studied during years.

In the present work, the use of photovoltaic panel is studied and the effect of applying tracking, concentration and cooling methods to improve the performance of the system is investigated. While using photovoltaic panels in the southeast Unites States has been judged less attractive than in other parts of the country owing to the humid climate and numerous cloudy days, in the present work the meteorological data are obtained from National Solar Radiation Database [1] for Tuscaloosa, Alabama and the annual performance of the system is determined for operation of the system in this area.

The combined use of photovoltaic cells and thermoelectric modules is another thrust of this research. Two innovative systems are proposed and investigated including combined photovoltaic-thermoelectric power generation system (PV-TEG) and combined photovoltaic-thermoelectric cooling system (PV-TEC). In the first system the TEG modules are considered to be installed in the backside of the PV panel to convert the excess heat from the PV cells to electricity. The performance of the system is evaluated under different conditions and by using

the meteorological data for Tuscaloosa, AL. In the second system (PV-TEC), two different approaches are proposed and investigated in order to use the combined PV-TEC system. In the first approach, the goal is keeping the cell temperature under a specific limit while in the second approach, the goal is maximizing the output power from the system by reducing the cell temperature. All the studies are performed via computer simulation in MATLAB and the results are discussed extensively through several graphs and tables.

DEDICATION

This thesis is dedicated to everyone who helped me and guided me through the trials and tribulations of creating this manuscript. In particular, my parents and my advisor who stood by me throughout the time taken to complete this work.

LIST OF ABBREVIATIONS AND SYMBOLS

A	surface area, m^2
C_P	specific heat, J/kg.K
G	solar irradiation, W/m^2
h	convective heat transfer coefficient, $W/K\ m^2$
I	electrical current, A
I_b	normal beam radiation intensity, W/m^2
k_B	Boltzman constant, 1.38×10^{-23} J/K
L	thickness, m
n	diode quality coefficient
P	power, W
q	electrons charge,1.602×10^{-19}C
Q_c	Rate of heat removal, W
Q_h	Rate of heat supplied, W
Q_{te}	electrically driven TEC power, W
R_{ha}	TEC hot side to ambient resistance, K/W
R_{jc}	junction to TEC thermal resistance, K/W
R_m	thermoelectric module electrical resistance, Ω
R	thermal resistance, K/W
S_m	Seebeck coefficient of thermoelectric module, V/K
T	Temperature, K
T_{sky}	sky temperature, K

Th	thickness, m
V	voltage, V
V_w	wind velocity, m/s
W	width, m

Greek

η_{el}	PV efficiency
ε_g	emissivity of PV panel
τ	transmissivity,
α	absorptivity
β	tilt angle
λ	site latitude
ρ_g	albedo of ground
ω	hour angle

Subsripts

a	ambient
b	base
bs	backside of tedlar
c	cell
d	diffuse
g	glass
h	horizontal

m	mean
max	maximum
mpp	maximum power point
oc	open circuit
sc	short circuit
ph	photocurrent
PV	photovoltaic
Ref	reference
si	silicon
sc	short circuit
T	tedlar
TEC	thermoelectric cooling module
TEG	thermoelectric generator module

ACKNOWLEDGMENTS

I am pleased to have this opportunity to thank many colleagues, friends, and faculty members who have helped me with this research project. I am most indebted to Dr. Keith Woodbury, my advisor and the chairman of the thesis committee, for sharing his research expertise and wisdom regarding motivational theory. I would also like to thank all of my committee members, Dr. John Baker and Dr. Muhammad Sharif, for their invaluable input and support of both the thesis and my academic progress.

This research would not have been possible without the support of my family who never stopped encouraging me to persist.

Contents

LIST OF TABLES

LIST OF FIGURES

CHAPTER 1: INTRODUCTION

Although fossil fuels are currently the most economical source available for power generation, the increasing price of oil and the harmful emissions generated due to combustion of fossil fuels have encouraged a lot of researchers to investigate economical methods for exploiting renewable energy sources all over the world. Solar energy is known as the most abundant source of energy on the earth. Using solar energy for power generation has been the focus of numerous researches during last decades. Solar energy can be converted to electricity either directly by using photovoltaic effect or indirectly by thermal storage and converting the stored thermal energy to electricity via heat engines. Each technology has its own advantages and drawbacks. However, the ease of installation, quiet and clean operation, and the scalability of the energy system are some features of PV panels which make them the most attractive option for residential applications.

Owing to the remarkable progress in material science and engineering, nowadays the cost of solar electricity has significantly decreased. However, it is still more expensive and less efficient than conventional power generation methods. Therefore, exploring methods to increase the conversion efficiency of solar power generation systems has great importance. The improvement in efficiency, especially in the multi-junction cells, has been remarkable over the last 20 years. There has been an increase in multi-junction cell efficiency of over 200% [2]. Figure 1 shows the best reported results for PV cell efficiencies from 1975 to 2010.

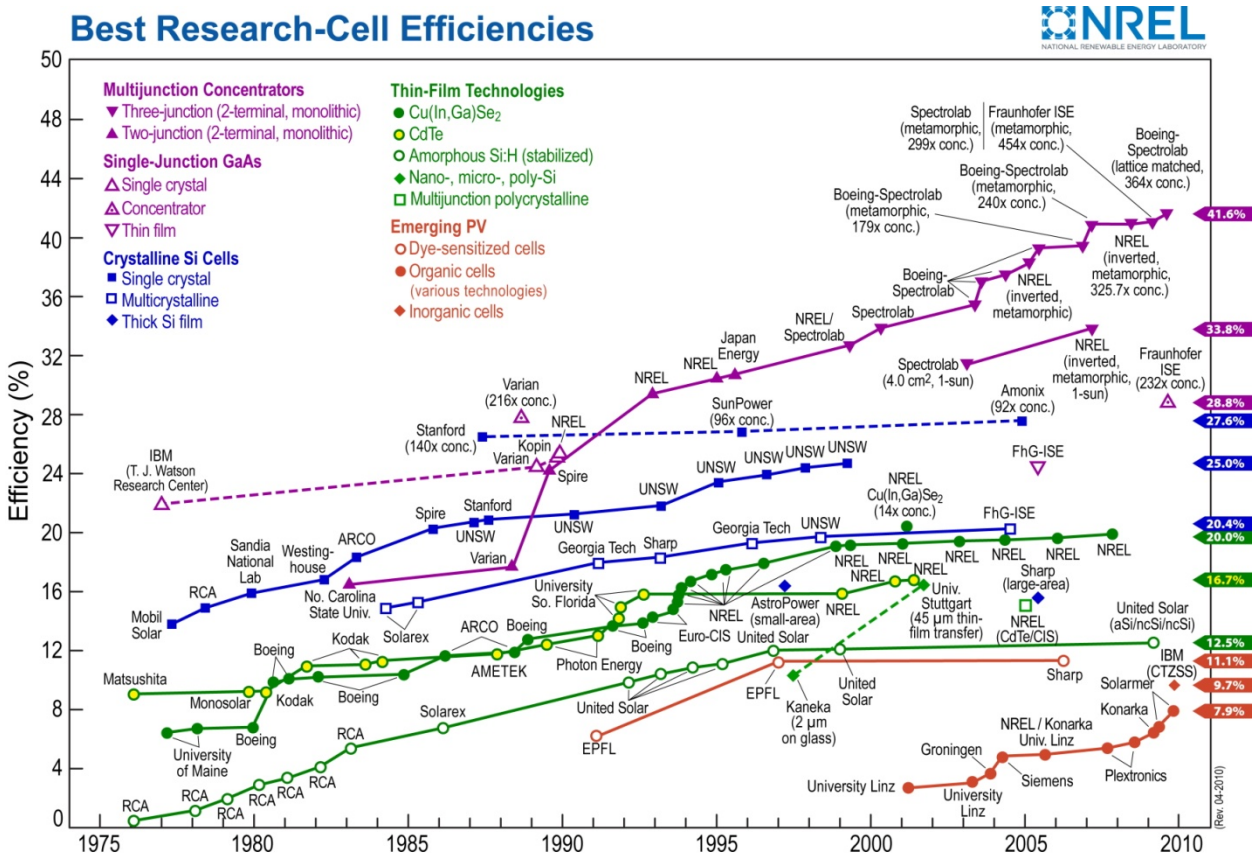

Figure 1: Best Reported PV Cell Efficiencies [2]

A review on photovoltaic technology, its power generating capability, the different existing light absorbing materials used, its environmental aspect coupled with a variety of its applications is presented by Parida et al [3].

Using different methods in order to increase the efficiency of solar power generation and make it a more cost effective technology have been studied during past years and various approaches have been introduced and tested. Sun tracking is one of these methods which can boost the total collected energy from sun by 10-100% [4]. Sun tracking systems move the solar panel based on hourly and seasonal movement of the sun in order to absorb the highest possible amount of energy. The sun-tracking systems could be passive or active and single or double axis. A review on sun-tracking methods is given by Mousazadeh [2]. Other alternative for cost

reduction in solar power generation is using mirrors, reflectors or lenses to concentrate the incoming solar radiation on the solar cell [5, 6]. Concentrating photovoltaics replaces expensive silicon solar cell with low-cost materials such as glass, mirror and plastic. This reduces the total solar cell area [7]. The concentrating photovoltaic systems (CPV) are categorized based on the amount of solar concentration into three groups including low, medium and high concentration. The low concentration photovoltaics can be achieved by simple mirrors which are cheaper, easier to install and more appropriate for smaller applications. A Review on modeling details of low-concentration photovoltaics is presented by Zahedi [8]. CPV systems operate efficiently in areas with a lot of direct sunlight, since diffuse light, which occurs in cloudy conditions, cannot be concentrated. In addition, as the concentration level goes higher, the necessity of using accurate tracking and appropriate cooling systems getting more important which adds to the capital cost of the system. The use of concentrating photovoltaic systems in different areas of the world has been studied [9] and tested [10].

Mallick et al. [11] designed and experimented a novel parabolic photovoltaic concentrator with different numbers of PV strings connected in series. They investigated the system both with and without concentrators and showed that the use of concentrator increased the maximum power point by 62% compared to a similar non-concentrating PV panel. Matsushima et al. [12] studied a concentrating solar module that is designed to achieve photovoltaic (PV) systems with higher generation power density with specific tilt angle and without tracking which resulted in increased electricity delivered by 1.5 times compared to conventional module. Huang et al. [13] proposed a one axis three position tracking PV module with low concentration ratio reflector. PV modules were mounted on a separate sun tracking

system where the one axis tracking mechanism adjusts the PV position only at three fixed angles in morning, noon and afternoon.

In 2010, OPEL Solar installed an HCPV (high concentration photovoltaic system) power plant with 330 kilowatts (kW) capacity in Spain with guaranteed investment rate of return. The system benefits from a dual axis tracker and can concentrate the solar radiation more than 500 suns onto high-efficiency multi-junction Ga-As solar cells [14].

Although concentration of solar direct beam on the PV cells can increase the output power, the temperature increment is an obstacle for efficiently performance of the system. Therefore, this usually necessitates using a proper cooling method. Several studies have been carried out to find the most efficient method for cooling photovoltaic panels including passive and active cooling methods [15, 16, 17, 18, 19]. Royne et al. [20] presented a comprehensive review on various methods for cooling photovoltaic cells. It has been suggested that for single cell, passive cooling works well enough and for densely packed cells under high concentrations more than 150 suns active cooling is necessary. Active cooling methods are generally more effective but more costly. The most common active cooling method is probably using photovoltaic-thermal collectors (PVT) which are basically solar panels with water or air channels passing from the back side of them. PVT systems have been widely studied since mid of 1970. A review on PVT systems is given by Chow [21]. The fluid which passes below the PV panel can reduces the cell temperature and while absorbs heat and gets warmer. The hot fluid (generally air or water) can be subsequently used for heating purposes or as the domestic hot water. This can add to the total efficiency of the system.

As already discussed, using photovoltaic panels owing to remarkable advances in material technology and efficient methods has started to be competitive in several places all over

the world and in west United States. However, it has been judged less attractive in the southeast United States owing to the humid climate and numerous cloudy days. Therefore, exploring the performance of a PVT system by using tracking and low concentration in Tuscaloosa, AL climate was one of the thrusts of this research. The system is modeled via MATLAB and a simulation is carried out to predict behavior of the system during different hours of the year by using weather data given in TMY3. A comprehensive heat transfer model is used considering different losses in order to determine the temperature through the system and calculate the output power accurately.

Although PVT collectors are very common, they have some issues such as potential leakage, pumping power, noisy operation and extra structural and maintenance cost. Therefore, exploring other alternatives for cooling solar panels can be useful. In the present work, the use of thermoelectric/Peltier effect are considered to explore the possibility of using thermoelectric cooling modules for cooling the PV panel and using thermoelectric power generator modules for harvesting the excess heat and convert it to power. Using combined PV-TEC is a novel idea and has not discussed in previous works and the concept of using hybrid PV-TEG system has been proposed by Sark [30].

The thermoelectric effect is the direct conversion of temperature differences to electric voltage and vice-versa. A thermoelectric device generates a voltage due to temperature gradient between each side. Conversely, applying a voltage to it results in a temperature gradient. Applying temperature gradient causes charge carriers in the material to diffuse from the hot side to the cold side. Studying the simultaneous use of thermoelectric modules and PV panels has been performed in few researches. PV technology can be used to provide the power for solar-driven thermoelectric refrigeration systems. Several studies have been performed to investigate PV thermoelectric cooling/refrigeration systems. A comprehensive review on these systems can

be found in [22]. Sample pictures from applications of thermoelectric modules are shown in Figure 2:

Figure 2: Thermoelectric modules and applications [23, 24, 25]

Using combined solar-thermoelectric systems has been discussed in some research works. Rockendorf et al [26] studied two different principles of thermoelectric cogeneration solar collectors: one is to combine a solar thermal collector with a thermoelectric generator (TEG) which delivers the electric energy and another approach is the combination of PV cells with a thermal collector and concluded that the second approach is more efficient. Vorobiev et al [27] described a system consisting of a radiation concentrator, photovoltaic cell, heat engine and thermoelectric generator. The possibilities of using semiconductor materials with different band gap values are analyzed and different thermoelectric materials considered. Tritt et al [28] discussed use of solar energy as the heat source for the thermoelectric power generation. A study on the potential benefits from the integration of PV and thermoelectric systems in mobile computing platform is performed by Muhtaroglu et al [29]. Recently, the idea of attaching

thermoelectric convertors to the back of PV modules to use the waste heat is proposed by Sark [30]. The result from his work shows that using PV-TE modules can potentially increase the annual energy yield by 14.7-11% for two annual irradiance and temperature profiles located in Malaga, Spain and Utrecht, Netherlands respectively. However, this work suffers from some inaccuracies due to over simplification of the model. Several heat losses have not considered including reflection losses. It is also assumed that the back side temperature of the TE converter always equals the ambient temperature which is not a very accurate assumption.

Another thrust, in the present work is the possibility of using combined PV-TEC and PV-TEG systems. A comprehensive model is developed to explore the benefits of using TEG modules connected to PV cells. TEG modules can convert a portion of excess heat generated out of the PV cells to electricity and increase the total efficiency of the system. In TEC case, a model is proposed in order to explore how effectively TEC modules can provide cooling for PV cells. The power to run TEC modules is provided by the PV panel itself. A comprehensive model is developed and coded in MATLAB in order to investigate the temperature distribution through the system and determine the output power. The performance of the system under different level of solar irradiation is investigated. Also, the annual performance of the system by using the meteorological data for Tuscaloosa, AL is analyzed and presented.

The results of this research presents the potential of using PV technology in South East United States and the effect of using tracking, concentration and cooling methods on the performance of the system. Moreover, the results provide a basis for evaluation of combined PV-TEC and PV-TEG systems and points out the potential benefits of using these systems.

CHAPTER 2: PHOTOVOLTAIC-THERMAL COLLECTORS

In this chapter, first an introduction on photovoltaic cells and photovoltaic effect is presented and afterwards the procedure for modeling the behavior of a photovoltaic-thermal (PVT) panel is illustrated. A comprehensive heat transfer model is developed and coded using MATLAB to simulate the behavior of the system. The model basically consists of two parts associated with thermal and electrical features of the PV panel. Weather data are obtained from TMY3 for Tuscaloosa, AL.

Photovoltaic Cells

Photovoltaics (PV) is a method for electrical power generation by converting solar radiation into electricity using semiconductors without using any heat engine. Photovoltaic devices are simple in design requiring very little maintenance. They can work as stand-alone systems to give outputs from microwatts to megawatts depending on the application. The application of photovoltaics is very wide including water pumping, remote buildings, solar home systems, communications, satellites, space vehicles and for large power plants. Owing to this capability, the demand for photovoltaics is increasing all over the world and has begun to become economically competitive with conventional energy sources [31].

The photovoltaic cell consists of at least two layers of semiconductor material, one with a positive and the other with negative charge. Some of the photons from the incidence sun light are absorbed by the semiconductor atoms which causes electrons of the semiconductor negative layer to be freed from the cell. The released electrons flow through a circuit and finally back into

the positive layer to complete the circuit. A schematic of the power generation in a photovoltaic cell is given in Figure 3.

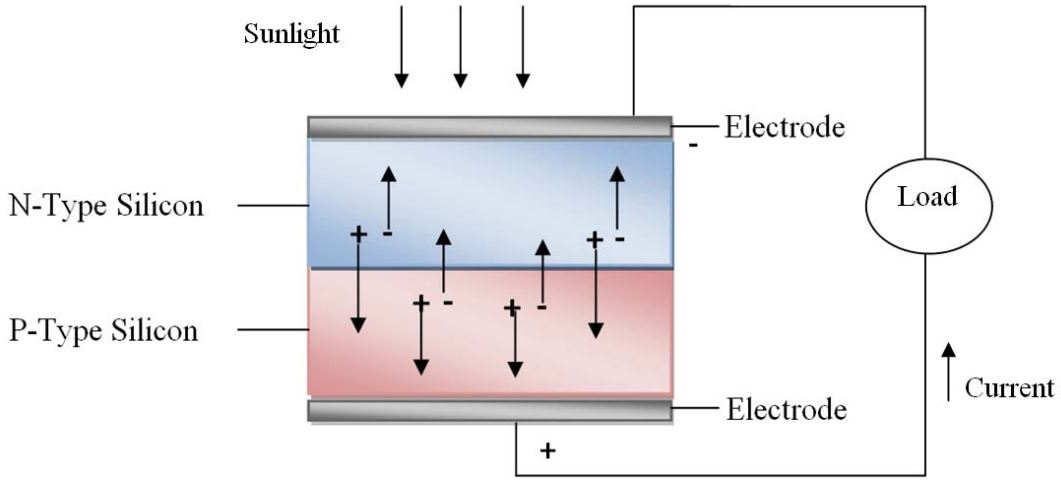

Figure 3: Schematic of power generation in PV cell

Scalability is one of the main advantages of using PV cells for power generation. Several individual PV cells can be connected together in a sealed, weatherproof package to create a "module". When two modules are wired together in series, their voltage is doubled while the current stays constant. Connecting two modules in parallel generates double amount of current while the voltage remains constant. Modules are wired in series and parallel into a "PV array" to achieve the desired voltage and current. The flexibility of the modular PV system allows designers to create solar power systems that can meet a wide variety of electrical needs [32].

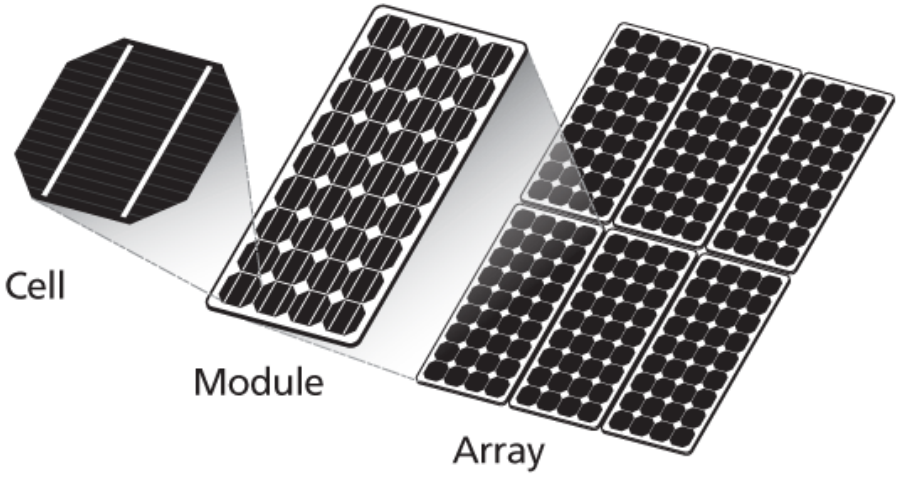

Figure 4: PV cell, Module and Array [33]

Solar cells based on silicon (Si) semiconductors account for nearly 90% of 2011 sales of photovoltaic (PV) products [34]. The main three silicon-based PV cells are monocrystalline, polycrystalline (multicrystalline) and thin film cells. Monocrystalline photovoltaic cells are cut from a single crystal of silicon and are the most common type of PV in the market. They have a higher efficiency than other two groups. They can be distinguished by their uniform appearance. Polycrystalline cells are cut from multifaceted crystalline silicon and are less efficient but less expensive than monocrystalline cells. Their appearance is more frosted looking and crystal-like. The thin film cells are the least efficient type out of these three but are much thinner than monocrystalline cells (monocrystalline cells are about 0.2 mm thick while the thickness of a thin film cell is only 2 micron). Although they have lower efficiency, they have one interesting advantage which is the possibility of making flexible panels which allow users to use them in different applications such as curved roofs and so forth. Figure 5 shows sample pictures from these three types of silicon based solar cells.

Figure 5: from left to right: Monocrystalline, polycrystalline and thin film PV cells

Concentrated Photovoltaics

Concentrated photovoltaics (CPV) is a rather new technology on the solar energy market today. CPV systems focus a large amount of sunlight onto a small area of solar photovoltaic materials to generate electricity. Therefore a much smaller CPV can produce power as much as a simple PV panel does by using concentrators. CPV systems operate efficiently with direct sunlight, as long as the solar cell is kept cool by using appropriate heat sinks. Cloudy areas which have a lot of diffused light and much less direct sun light are not appropriate for CPV installation since the diffused sun light cannot be concentrated.

Different methods and tools are utilized for concentrating solar radiation on PV cells. These tools could be simple mirrors, Fresnel lenses, or other types of reflectors. Low concentration photovoltaic modules use mirrors to concentrate sunlight onto a solar cell. The angle of the mirrors depends on the inclination angle, latitude and the module design. The Fresnel lens consists of a set of concentric annular sections and needs less material compared to a

conventional spherical lens. Fresnel lenses can be in circular or cylindrical shapes and are capable of concentrating the sunlight up to 500 suns. There are also several other methods for concentrating sunlight such as using parabolic mirrors and luminescent concentrators each of which could be used for different applications. Figure 6 shows a schematic of some of the most common concentrating methods.

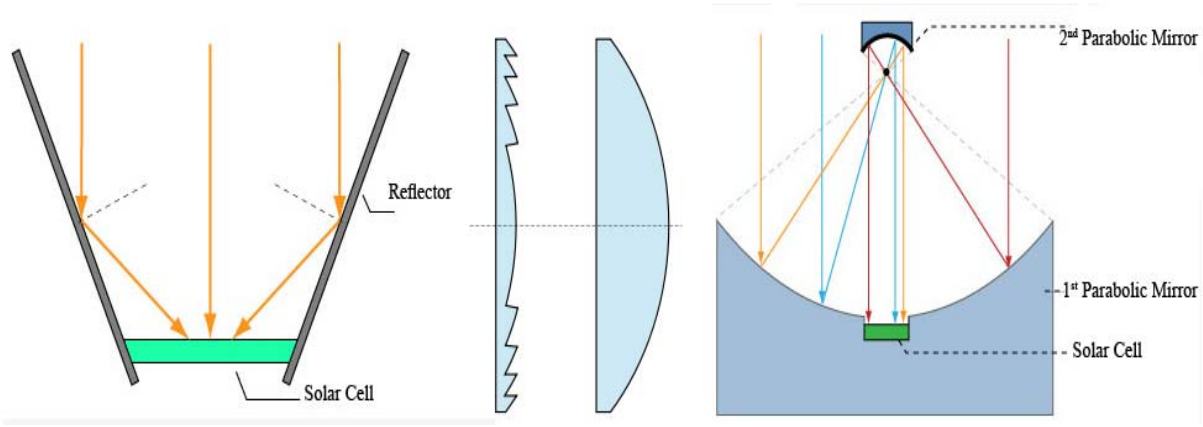

Figure 6: From left to right: A schematic of reflectors, Fresnel and conventional lens and parabolic mirrors [35, 36]

Photovoltaic-Thermal Collectors (PVT)

PV panels convert solar energy to electricity with ideal conversion efficiency in the range of 15 % and the rest of the solar energy is wasted as heat which is not utilized. This heat increases in the operating temperature of the PV cell which in turn results in a significant reduction in the overall performance of the PV cells. The solar cells can be either passively (e.g. through fins) or actively cooled (with a fluid stream like air or water) and this can increase the electricity generation. However, the total conversion efficiency could be higher if one would make use of the extracted heat. Hybrid photovoltaic-thermal (PVT) collector system is a

combination of photovoltaic and solar thermal components which produces both electricity and heat at the same time from the same surface area. PV modules can operate at almost 50 ºC above the ambient temperature which can reduce the efficiency of the panels by 25% (typically 0.4% per degree C rise for c-Si cells). Numerous correlations expressing cell temperature and efficiency as functions of the corresponding weather variables and cell working conditions are summarized by Skoplaki and Palyvos [37, 38]. By dissipating the heat from the PV panels, the efficiency of the power generation system is remarkably increased and on the other hand this heat can be utilized for different purposes such as providing domestic hot water and heating demands of the building.

For real-building project applications, the PVT collectors with air as the coolant were more readily adopted in the European and North American markets although the higher efficiency of the water-cooled system has been confirmed [39].

PVT Model

In the present work, a PVT system with air as coolant fluid is considered and modeled via MATLAB. A heat transfer model is required to simulate the behavior of the system which is discussed in this section. The meteorological data including solar radiation parameters, ambient temperature and wind velocity are obtained from TMY3 database.

A schematic of the considered system is given in Figure 7. Only a small portion of the available sunlight on the PV panel converts to electricity and the rest of it will dissipate as heat. On the top surface of the panel, heat losses occurr through conduction, convection and radiation. At the bottom of the PV cells, heat transfers from the solar cells to the tedlar through conduction.

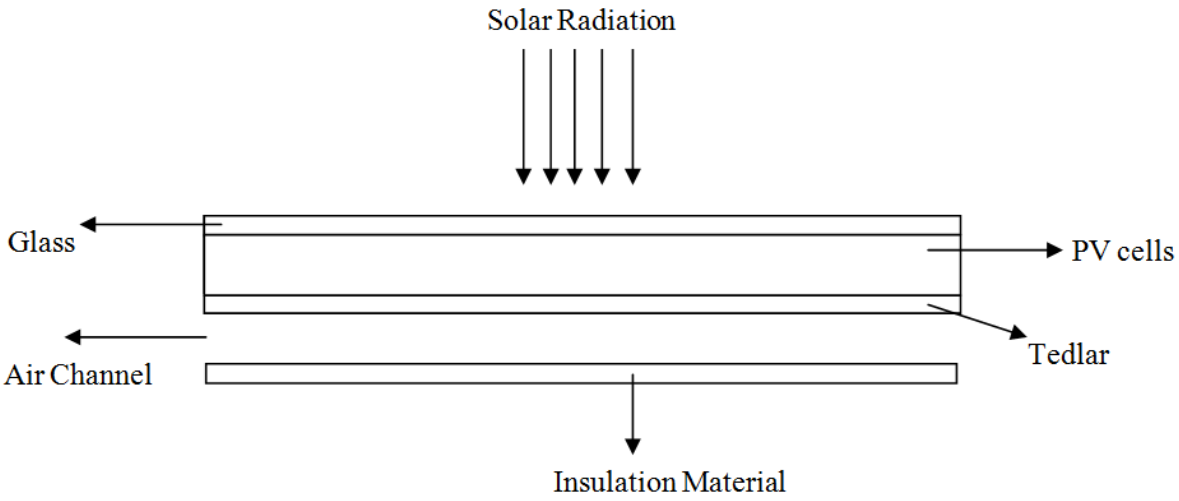

Figure 7: Schematic of the PVT system

The rate of solar energy available on PV panel is equal to the sum of the overall heat loss from the top surface of PV cell to the ambient including radiative, convective and conductive losses, the overall heat transfer from the PV cell to the back surface of tedlar and the rate of electrical energy produced [40]:

$$\tau_g \left[\alpha_c \beta_c G + \alpha_T (1-\beta_c) G \right] A_{PV} = U_t \left(T_{cell} - T_{amb} \right) A_{PV} + \varepsilon_g \sigma A_{PV} \left(T^4{}_{cell} - T^4{}_{sky} \right) + U_T \left(T_{cell} - T_{bs} \right) A_{PV} + \tau_g \beta_c \eta_{el} G \, A_{PV} \quad (1)$$

In this equation, the left side is the available solar energy on the PV panel. Where τ_g is the transmissivity of the glass, α_c and α_T represented the absorptivity of the solar cells and the tedlar respectively and β_c refers to the packing factor of the solar cell. The packing factor can be defined as the fraction of absorber plate area covered by the solar cells.

On the right hand side, the first term refers to the convective and conductive heat losses through the top of the panel, the second term is the radiative loss from the top side, the third term shows the conductive heat transfer from the cell to the back surface of tedlar and finally the last term represents the portion of the sunlight which converted to electricity. Where ε_g is the emissivity of the PV panel, σ is the Stefan-Boltzmann constant and is equal to 5.6703×10^{-8} (W/m^2K^4) and η_{el} is the electrical efficiency of the PV panel. The conductive heat transfer coefficient, U_T, from solar cell to ambient through tedlar is defined by:

$$U_T = \left[\frac{L_{si}}{K_{si}} + \frac{L_T}{K_T} \right]^{-1} \quad (2)$$

The overall heat transfer coefficient from solar cell to ambient through glass cover, U_t, which includes conduction and convection losses can be given as:

$$U_t = \left[\frac{L_g}{K_g} + \frac{1}{h_{conv,t}} \right]^{-1} \quad (3)$$

Sky temperature is defined as the temperature at which the sky (as a blackbody) emits radiation at the rate actually emitted by the atmosphere at ground-level temperature with its actual emittance. The atmosphere emittance is a complex function of air temperature and moisture content. However, by ignoring the vapour pressure of atmosphere, following equation can be used to estimate the effective temperature of the sky (T_{sky}) [41]:

$$T_{sky} = 0.0552 \times T_a^{1.5} \tag{4}$$

The convective heat transfer coefficient from the top of the PV panel, $h_{conv,t}$, which can be calculated by determining the Nusselt number for the external flows considering the size of the panel and wind velocity as below [42]:

$$\mathrm{Re} = \frac{VL}{\upsilon} \tag{5}$$

$$\mathrm{Nu} = 0.102 \times \mathrm{Re}^{0.675} \times \mathrm{Pr}^{\frac{1}{3}} \tag{6}$$

$$h_{conv,t} = \frac{Nu \times K}{L} \tag{7}$$

In most of the previous works, the value of convective heat transfer coefficient is considered a constant average value or simplified correlations are used for calculations [40].

An energy balance equation can be also written for the back surface of tedlar:

$$U_T \left(T_{cell} - T_{bs}\right) A_{PV} = \mathrm{h}_a \left(T_{bs} - T_m\right) A_{PV} \tag{8}$$

The term in the right hand side refers to the removed heat by convection between the tedlar and the flowing air. The value of h_a or the convective heat transfer coefficient between the

tedlar and flowing air is calculated by using the appropriate correlation for internal flows through a duct as below [42]:

$$\mathrm{Nu}=0.0243\times \mathrm{Re}^{\frac{4}{5}}\times \mathrm{Pr}^{\frac{1}{3}} \tag{9}$$

The third equation can be written based on the energy balance for the air flowing through the channels.

$$\dot{m}C_P\left(T_{out}-T_{in}\right)+U_b\left(T_m-T_{amb}\right)A_{PV}=h_a\left(T_{bs}-T_m\right)A_{PV} \tag{10}$$

It should be noted that an average mean temperature is considered as the fluid temperature through the ducts:

$$T_m=\frac{T_{in}+T_{out}}{2} \tag{11}$$

The overall back loss coefficient from flowing air in channel to ambient air can be found as:

$$U_b=\left[\frac{L_i}{K_i}+\frac{1}{h_a}\right]^{-1} \tag{12}$$

The system of three equations (1, 8 and 10) with the three unknowns T_{cell}, T_{bs}, T_{out} is solved via MATLAB for every hour based on the weather data for Tuscaloosa, AL.

Electrical Model

Obtaining the cell temperature leads to the next step which is calculation of the generated power via PV cell. An explicit model proposed by Saloux et al. [43] is utilized as discussed

below. The proposed expressions, based on explicit methods, allow the current and the voltage at key operational points, (i.e., in particular at the maximum power point) to be calculated using the single-diode model as a function of cell temperature, irradiance and common manufacturers data.

Some of the main parameters are defined before explaining the model. Figure 8 shows a typical I-V curve for a PV cell.

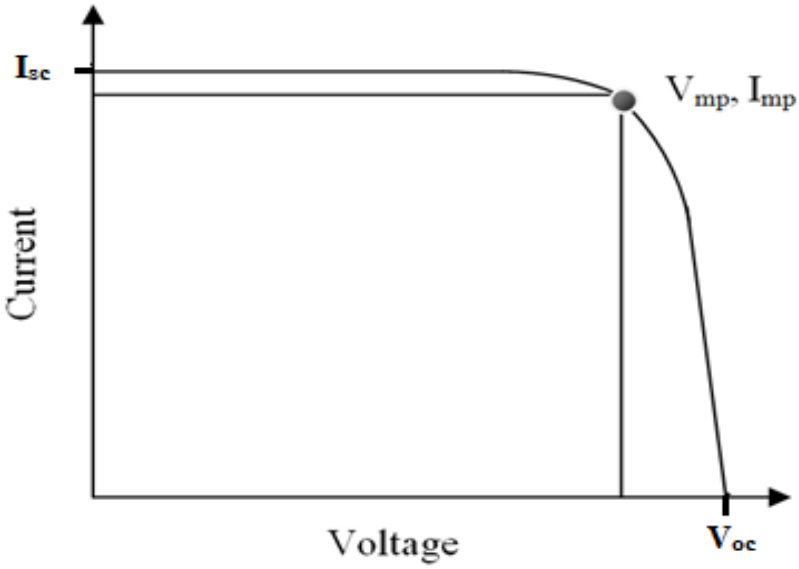

Figure 8: Typical IV curve of a PV cell

A current-voltage (I-V) curve shows the possible combinations of current and voltage of PV cell. A PV cell produces the highest current when there is no voltage which means when there is a short circuit between its positive and negative sides (no resistance). The maximum possible current is called as the short circuit current (I_{sc}). At this current, the voltage across in the circuit is zero.

The maximum voltage is called the open circuit voltage (V_{oc}) which happens when the resistance is very high. In this case the circuit is incomplete and the current is zero. These two

extremes in load resistance, and the whole range of conditions in between them, are demonstrated on the I-V curve (Figure 8).

The power available from a PV cell at any point along the curve is the product of current and voltage at that point and is expressed in Watts. At both short circuit current point and open circuit voltage point the output power is zero. There is a point on the knee of the curve where the maximum power output is located, the corresponding voltage and current are called maximum power point voltage and maximum power point current.

The equivalent electrical circuit for a PV cell can be based on single- or double-diode ideal PV cell models. Here we considered the single diode model without internal resistances which is proved to be accurate enough. A schematic of the considered circuit is shown in Figure 9.

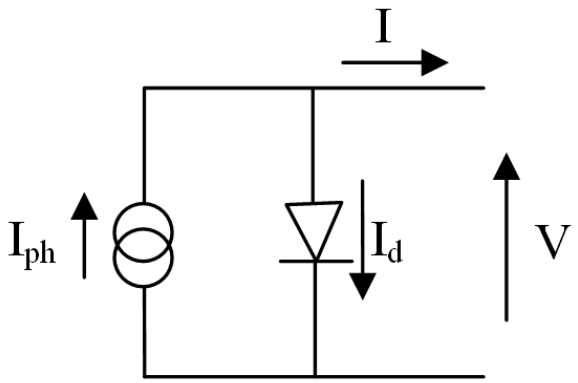

Figure 9: Equivalent single diode electrical circuit for PV cell

The photocurrent as a function of irradiance and temperature can be found as:

$$I_{ph} = \frac{G}{G_{ref}}\left[I_{ph,ref} + \mu_f \left(T - T_{ref} \right) \right] \tag{13}$$

The saturation current can be written based on the short-circuit current temperature coefficient as well as the open-circuit voltage temperature coefficient:

$$I_o = \frac{I_{sc,ref} + \mu_f \left(T - T_{ref}\right)}{\exp\left[\frac{q\left(V_{oc,ref} + \mu_V \left(T - T_{ref}\right)\right)}{nN_s k_B T}\right] - 1} \tag{14}$$

Where q is the elementary charge equal to 1.6×10^{-6} Coulombs, μ_I and μ_V are current temperature coefficient (A/K) and voltage temperature coefficient (V/K) respectively. Finally, n is the diode quality coefficient and can be determined as:

$$n = \frac{q\left(V_{m,ref} - V_{oc,ref}\right)}{N_s k_B T_{ref}} \frac{1}{\ln\left(1 - \frac{I_{m,ref}}{I_{sc,ref}}\right)} \tag{15}$$

Therefore, the voltage and the current at the maximum power point and the corresponding power can be found as follow:

$$V_{mpp} = \frac{nN_s k_B T}{q} \ln\left(\frac{nN_s k_B T}{qI_o} \frac{I_{sc}}{V_{oc}}\right) \tag{16}$$

$$I_{mpp} = I_{ph} + I_o - \frac{nN_s k_B T}{q}\left(\frac{I_{sc}}{V_{oc}}\right) \tag{17}$$

$$P_{mpp} = I_{mpp} V_{mpp} \tag{18}$$

Where the open circuit voltage can be given as below:

$$V_{oc} = \frac{nN_S k_B T}{q} \ln\left(1 + \frac{I_{sc}}{I_o}\right) \tag{19}$$

Weather Data

For this research, the climate of Tuscaloosa, AL is considered as the base case and the necessary hourly information is obtained from TMY3 prepared by National Solar Radiation Data Base (NSRDB) update [44]. The TMY datasets hold hourly values of solar radiation and meteorological elements for a 1-year period. Their intended use is for computer simulations of solar energy conversion systems and building systems to facilitate performance comparisons of different system types, configurations, and locations in the United States and its territories. Using solar energy in east coast US has not grown as much as west coast owing to the humid weather and numerous cloudy days. One purpose of this research to provide a good view on solar energy potential in east coast US and particularly in Tuscaloosa, AL.

Figure 10 shows the annual temperature profile in Tuscaloosa, AL. As can be seen, the temperature varies between 264 K and 310 K during the whole year and the highest temperature occurs in mid August.

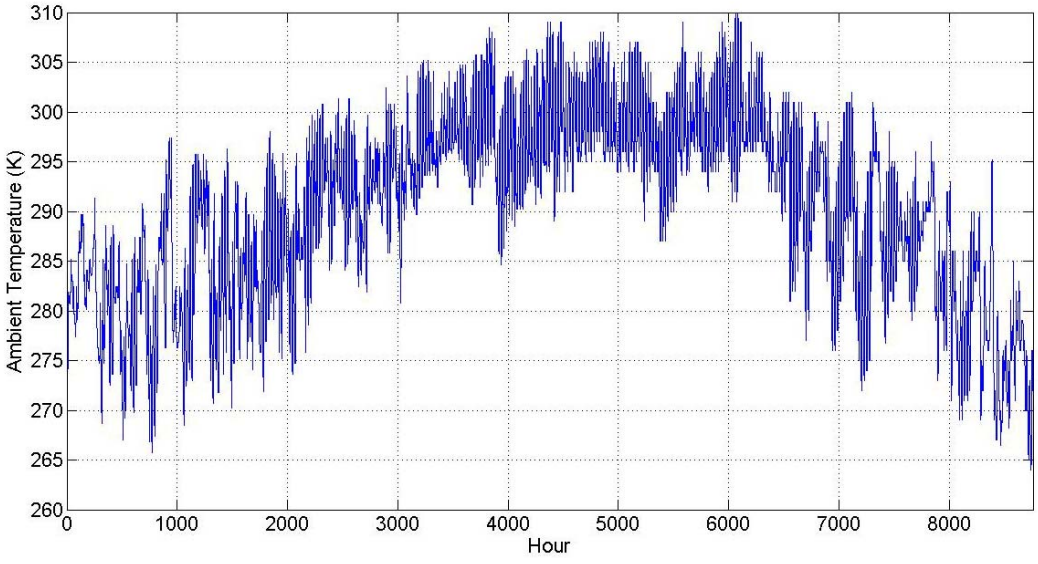

Figure 10: Annual temperature profile for Tuscaloosa, AL

The ambient temperature is one of the factors which needs to be considered for calculating the temperature through the PV panel and the generated output power.

In order to do analysis on solar cells and calculate the generated power, the total collectible solar radiation needs to be determined. When the solar radiation passes through the earth's atmosphere, parts of it is absorbed or scattered by air molecules, water vapor, aerosols, and clouds. The part of radiation which passes through directly to the earth's surface is called Direct Solar Radiation and denoted by I_b in this work. The radiation that has been scattered out of the direct beam is called Diffuse Solar Radiation which is specified by I_d here. The direct component of sunlight and the diffuse component of skylight falling together on a horizontal surface make up Global Solar Radiation (I_h).

The variation of direct solar radiation and diffuse solar radiation in the period of one year are shown in Figure 11 and Figure 12 respectively. The average daily direct solar radiation for the Tuscaloosa area is 3575.5 W-hr/m^2-day which is not very high in compare with some other areas such as Arizona with about 7000 W-hr/m^2-day, but is literally in an acceptable level to make use of it. It should be noted that, unlike non-concentrating PV systems, , concentrating solar systems can only use the direct part of the solar radiation and just a small portion of diffuse light.

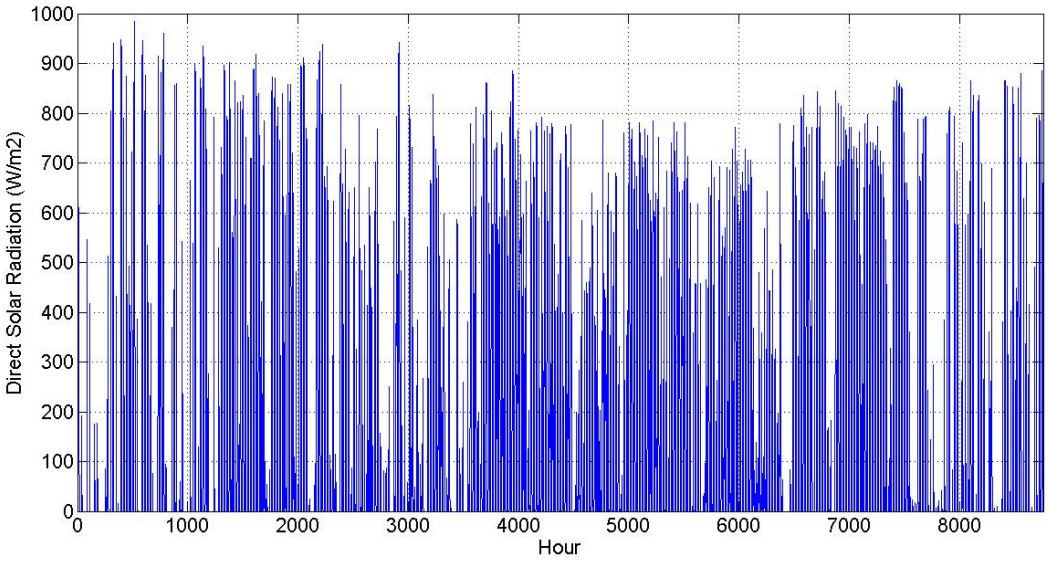

Figure 11: Direct solar radiation profile- Tuscaloosa, AL [1]

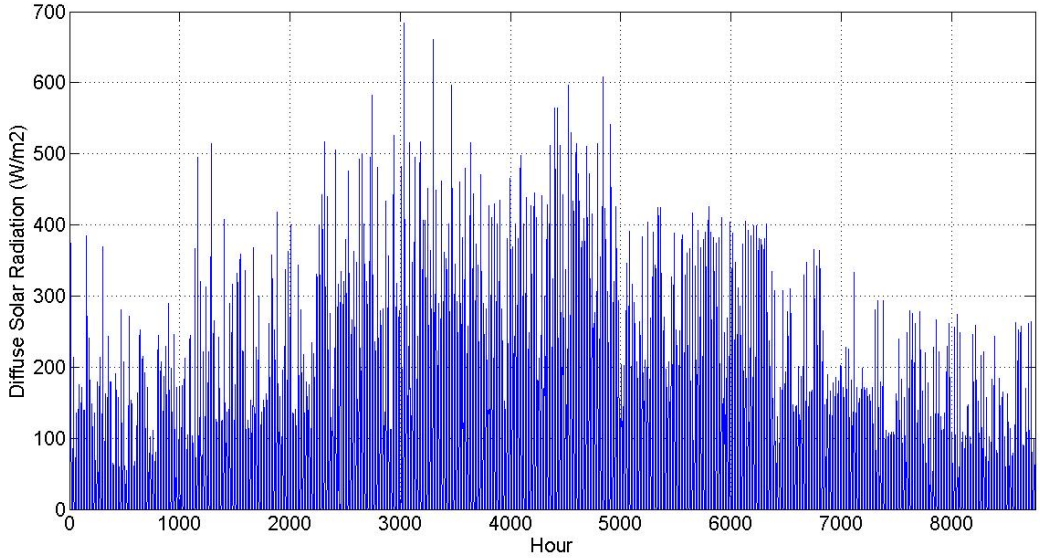

Figure 12: Diffuse solar radiation- Tuscaloosa, AL [1]

In the next step, the hourly collectible solar radiation is calculated for three different cases: without tracking, with one axis tracker and with double axis tracker. Following is the procedure for finding the value of hourly collectible radiation (G) on fixed solar panels.

Considering a constant tilt-angle, β_0, from the horizon, the collectible radiation can be determined by summing the contribution of the direct beam radiation, the component of sky diffuse radiation, and the radiation reflected from the ground as below [45]:

$$G = f \times I_b \cos\theta_0 + H_d R_d + \rho_g H_h \left(1 - \cos\beta_0\right)/2 \tag{20}$$

where H_d and H_h are hourly sky diffuse and hemispherical radiation on horizon respectively, R_d represents the ratio of the daily sky diffuse radiation on unit area of the tilted surface and θ_0 is the incidence angle of solar rays on a south-facing tilted surface.

The values of R_d and θ_0 can be found as [46]:

$$R_d = \frac{\left(2 + \cos\beta_0\right)}{3} \tag{21}$$

$$\cos\theta_0 = \cos\theta_z \cos\beta_0 + \left(\cos\delta\cos\omega\sin\lambda - \sin\delta\cos\lambda\right)\sin\beta_0 \tag{22}$$

where λ is the site latitude, θ_z is the incidence angle of solar rays on the horizon and δ is the declination of the sun in the nth day of the year (counted from the first day of January). The unknown angles can be determined by following equations:

$$\cos\theta_z = \cos\delta\cos\lambda\cos\omega + \sin\delta\sin\lambda \tag{23}$$

$$\sin\delta = -\sin 23.45 \cos\left[360\left(n+10\right)/365.25\right] \tag{24}$$

$$\cos\omega_0 = -\tan\delta\tan\lambda \tag{25}$$

It should be noted that f in Eq. 1 [45] is equal to 1 for $\cos\theta_0 \geq 0$ and is equal to 0 for $\cos\theta_0 < 0$.

Tracking

One of the issues in using solar energy is the position of sun which varies during the day and as a result the value of collectible energy changes. Several studies have been performed in order to find the optimal tilt angle and azimuth angle for installing the PV panel in order to collect the most possible energy in each location. It has been mentioned in several references that the rule of thumb is that the optimal tilt angel is almost equal to the value of latitude of the location. However, recently a more accurate research by Kleissl et al [47] determined the value of optimal tilt angle for different locations in United States which shows that the rule of thumb could be wrong by about 10 degrees. Based on this research, the optimal angle for Tuscaloosa, AL is almost 2 degrees more than the latitude (33.2) and is about 35 degrees. Although placing the solar panel at an optimum angle can increases the value of total collectible energy and generated power, sun-tracking methods can definitely improve the total efficiency of the system by collecting maximum possible energy. The solar tracker is a device that keeps PV in an optimum position perpendicular to the solar radiation during daylight hours which could be single or double axis. Single axis trackers have one degree of freedom that acts as an axis of rotation while dual axis trackers have two degrees of freedom that act as axes of rotation which these two axes are usually normal to each other. Calculating the hourly collectible radiation on a 2-axis tracked panel is given below [45]:

$$G_{2axis} = \left[I_b + I_d \left(2 + \cos\beta_2\right)/3 + \rho_g I_h \left(1 - \cos\beta_2\right) \right] \tag{26}$$

where I_d and I_h are instantaneous diffuse and globe radiation on the horizon respectively, β_2 is the tilt angle of the full two axis tracked panel from the horizon which is equal to the zenith angle of the sun ($\beta_2 = \theta_z$).

Hourly collectible radiation on the single axis tracked panel can be found as [45]:

$$G_{1,axis} = \left[I_b \cos\theta_1 + I_d \left(2 + \cos\beta_1\right)/3 \right] + \rho I_h \left(1 - \cos\beta_1\right)/2 \tag{27}$$

where θ_1 is the incidence angle of solar rays on the single axis tracked panel and β_1 is the tilt angle of the tracked panel relative to the horizon. Here a coordinate system is defined to calculate these two angles. In this coordinate system the Z-axis is parallel to the tracking axis and pointing to the northern sky dome, Y- axis pointing to the east and X-axis pointing to the southern sky dome. The unit vector from the earth to the sun can be shown as [45]:

$$n_S = \left(n_x, n_y, n_z\right) \tag{28}$$

where

$$n_x = \cos\delta\cos\omega\cos\left(\lambda - \beta_{SN}\right) + \sin\delta\sin\left(\lambda - \beta_{SN}\right) \tag{29}$$

$$n_y = -\cos\delta\sin\omega \tag{30}$$

$$n_z = -\cos\delta\cos\omega\sin\left(\lambda - \beta_{SN}\right) + \sin\delta\cos\left(\lambda - \beta_{SN}\right) \tag{31}$$

where β_{SN} is the tilt angle of single axis tracker to the horizon and considered equal to site latitude plus or minus the deviation value from [47]. Now, the value of β_1 can be calculated as:

$$\cos\beta_1 = n_c . n_h = \frac{n_x \cos\beta_{SN}}{\sqrt{{n_x}^2 + {n_y}^2}} \tag{32}$$

Simulation and Results

The properties of the selected PV panel are given in Table 1. The considered PV panel is a Siemens SP75, mono-crystalline silicon with air channel installed on the back side of it. The air blows in to the duct underneath of the solar panel which provides cooling effect for the PV cells.

Table 1: PV panel characteristics

Parameter	Value
$I_{m,ref}$	8.8
$V_{m,ref}$	8.5
$I_{sc,ref}$	9.6
$V_{oc,ref}$	10.9
NOCT	45
μ_f , current temp. coeff.	2.06 mA/C
μ_V , voltage temp. coeff.	-0.077 V/C
Dimensions	1200× 527× 34 mm
η_{el}	12%
L_{si} , thickness of silicon solar cell	300×10^{-6}
K_{si} , conductivity of silicon solar cell	0.036W/mK
L_g , thickness of glass cover	0.003 m
K_g , conductivity of glass cover	1 W/mK
τ_g , transmissivity of glass cover	0.95
ε_g , emissivity of PV	0.88
α_T , absorptivity of tedlar	0.5
L_T , thickness of tedlar	0.0005 m
K_T , conductivity of tedlar	0.033 W/mK
V_W , wind velocity	2 m/s
L_i , thickness of back insulation	0.05 m
K_i , conductivity of back insulation	0.035 W/mK

A schematic of the simulated system is shown in Figure 13.

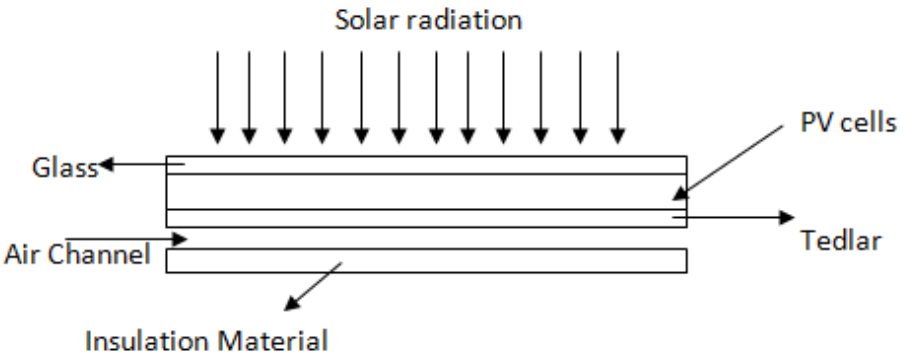

Figure 13: Schematic of the simulated PVT system

A simulation is carried out to investigate the responses of the model under different levels of solar radiation prior to the simulation for the Tuscaloosa weather data. The variation of cell temperature and tedlar backside temperature with solar radiation is depicted in Figure 14

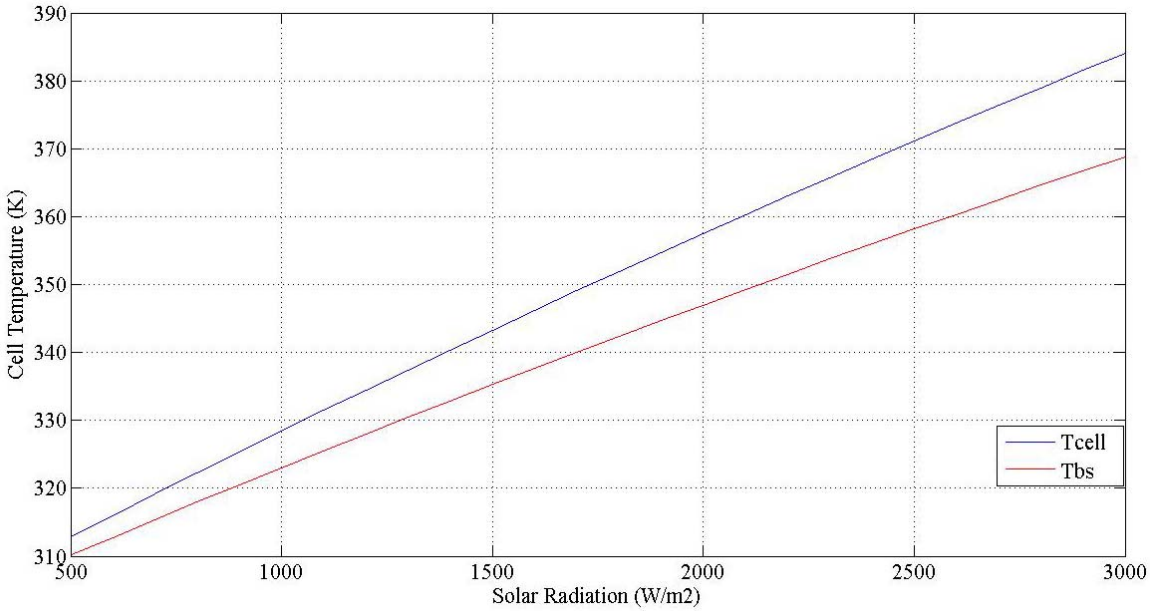

Figure 14: Variation of cell temperature and tedlar backside temperature with solar radiation

The temperature at different values of wind speed and solar radiation is then determined and compared with experimental data given in [48] on the same solar panel. The results show a

good correspondence between the simulation results and the experimental data. A summary of these simulations is given in Table 2.Table 1

Table 2: Comparison of experimental data with the simulation results

Solar Radiation (W/m^2)	T_{in} (K)	T_{amb} (K)	T_{cell} (K) experimental	T_{cell} (K) simulation	T_{bs}(K) experimental	T_{bs} (K) simulation	V_{wind} (m/s)
409.63	33	30	41.1	42.7	42.9	41	1.98
535.5	34.9	32	47.9	50	46.8	48.1	1.42
658	42.3	38	54.9	59.2	57.2	56.5	1.73
253.75	40.8	40	47.2	46.6	46.4	45.5	1.83

The effect of cell temperature under different solar radiation intensity on generated power by the PV cell is illustrated in Figure 15.

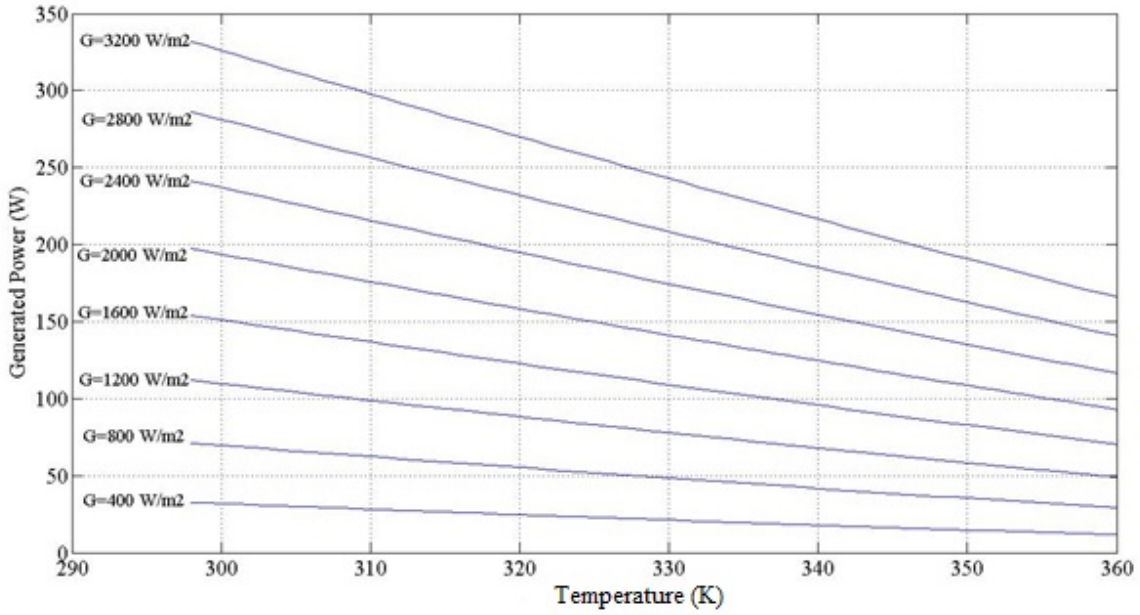

Figure 15: Variation of generated power by PV cells versus cell temperature under different solar radiation level

It can be seen that the generated power by the PV cell decreases by increasing cell temperature. This effect is much more sensible at higher solar radiation. This clearly shows the necessity of an appropriate cooling system for concentrated PV systems.

In the next part of simulation, the considered PV panel is tested under meteorological data for Tuscaloosa, AL. The effect of using tracking, concentration and cooling is also analyzed and discussed extensively.

In Figure 16 the effect of using tracking methods is investigated. The three scenarios including a system without tracking, single axis tracking and double axis tracking are considered and in each case the total value of daily collectible radiation (without concentration) is plotted.

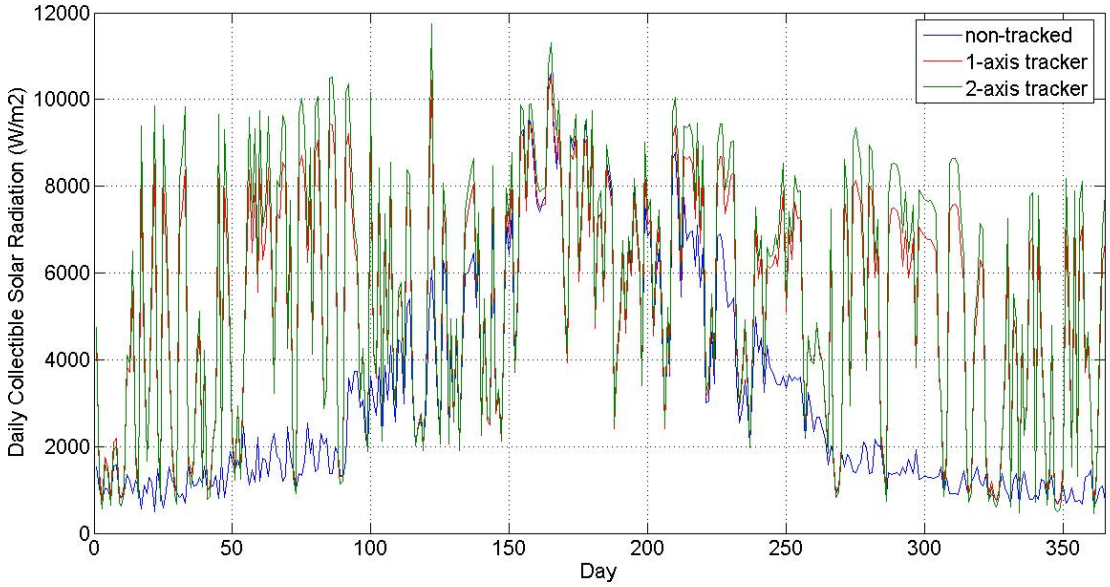

Figure 16: Daily collectible radiation and the effect of sun tracking

The total annual collectible radiation by using a system without tracking is about 68% less than the system with one axis tracking and 78% less than the system with double axis tracking. As can be seen there is a significant difference between the system without tracking and

the one which benefits from a single axis tracking system. However, it can be seen that using a double axis tracking does not make a remarkable difference compared to the single axis tracking.

Single axis trackers can track the sun from east to west on a single pivot point while double axis trackers track east to west and tilt for north to south tracking. Double axis trackers are much more complex in design than single axis trackers and necessitate more maintenance cost. Therefore, for typical applications and in low concentration levels, single axis tracker systems are more suitable option.

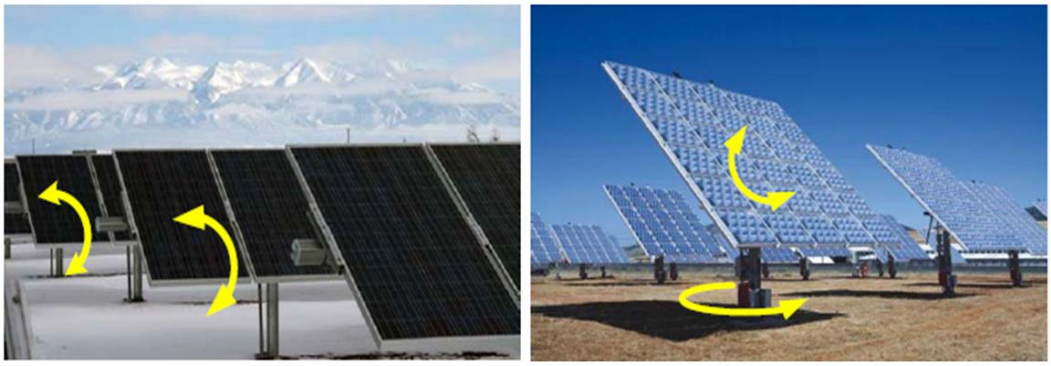

Figure 17: single axis and double axis tracker for PV applications [49]

By increasing the total collectible radiation on solar panels, it is possible to generate more power. Figure 18 shows a comparison chart between the generated power for a system which is fixed at the optimal tilt and a system with single axis tracking during a year. It can be seen that during the summer, when the best tilt angle is very close to the optimal yearly tilt, the generated power via both systems is almost close. However, other than the summer period, there is a significant difference between the generated power by the system with a single axis tracker and the system without tracking. It is found that by using a single axis tracking system, 133 kWh/yr energy could be produced by the considered solar panel which is 60.9% more than the system without tracker.

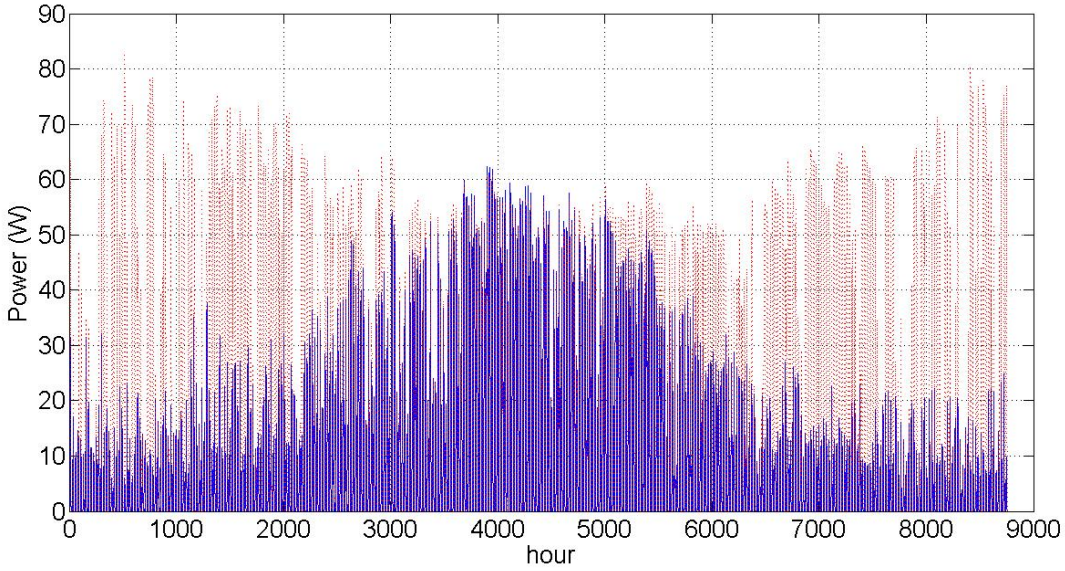

Figure 18: Effect of single axis tracking on generated power by PV panel

Concentration

Concentration of sun on the PV cells is another way to increase the output power out of the same surface area. Concentrating photovoltaic systems (CPV) mainly using the direct sun light and therefore would need a tracking method specially for high concentration levels. Moreover, due to the rises in cell temperature, an appropriate cooling method would be needed if the concentration would exceed a certain level in order to prevent the efficiency loss and long term degradation of the cells. The concentrator could be lenses or mirrors. For low level concentrations, mirrors can works properly and with a cheaper price. In Figure 19 a schematic of a simple 2X CPV module is demonstrated.

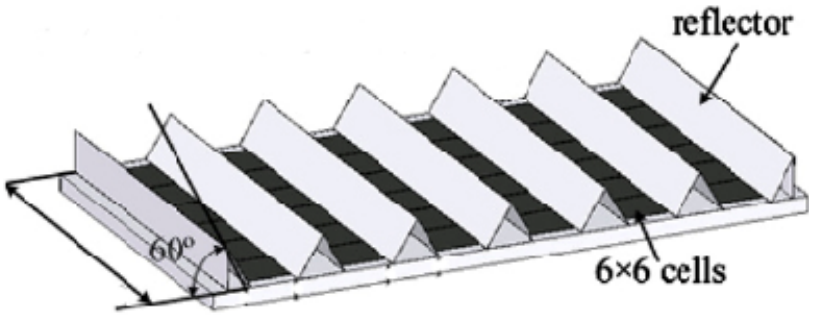

Figure 19: Schematic of a 2X CPV panel [50]

In Figure 20 the effect of using concentration on the cell temperature is presented. Low level concentration is fairly cheap and easy to implement with mirrors. A system with low concentration level of 2x which benefits from a single axis tracker is simulated and compared with a system without concentration and tracking.

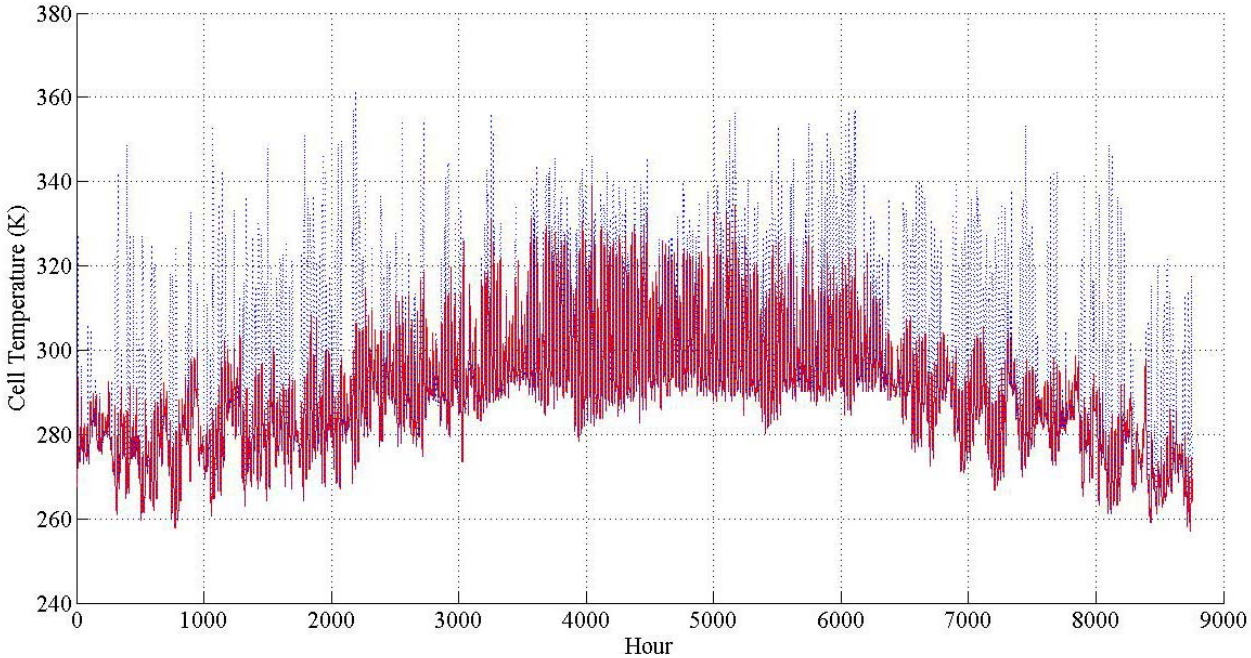

Figure 20: Effect of low level concentration (2x) on cell temperature

As can be seen in Figure 20, the cell temperature while using concentration consistently increases and goes up to about 360 K in hot season. As it is already discussed, higher temperature would decrease output power.

Figure 21 shows a comparison between generated power by the system which uses 2x concentrator and a single axis tracker versus a basic system without tracking or concentration. It is determined that the total energy generated by the improved system (165 kWh/yr) is about as twice as the basic system (82 kWh/yr). This clearly shows the significant effect of using tracking and concentration equipments on the generated power by the solar panels. It should be noted that the CPV systems accept the direct component of the incoming radiation and therefore must be oriented appropriately to maximize the energy collected. Therefore, using a tracker would be very effective to track the sun and collect more direct sunlight for the CPV system.

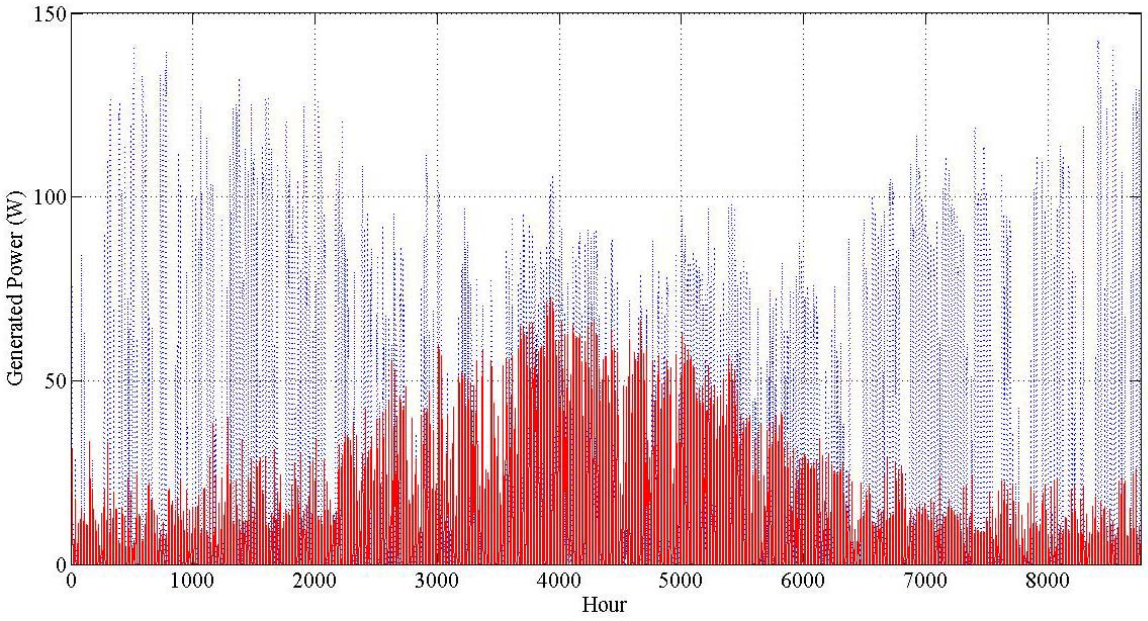

Figure 21: Generated power by the CPV system with 1 axis tracker and a simple PV panel

As it has already been mentioned, higher cell temperature would result in less output power and therefore, it is indeed desirable to use an appropriate cooling system for the solar

panel to keep it at the recommended range. In this study, it is proposed that an air channel be installed in the back side of the solar panel to remove some of the heat load from the PV panel. The air moves through the channel with the speed of 4 m/s and with the same temperature as the ambient. Figure 22 shows the annual cell temperature profile for a 2x CPV system with and without cooling. The red line shows the system without cooling and the blue line represents the simulation results for the system with cooling. As can be seen, by using air channels, the cell temperature does not exceed 340 K at the worst case. The lower temperature, results in higher output power which is demonstrated in Figure 23. It is determined that the CPV system with cooling can generates 177 kWh/yr which is about 7.3% more than the system without cooling. This shows the importance of using appropriate cooling method for CPV systems. It can also prevent from long term degradation of the cells.

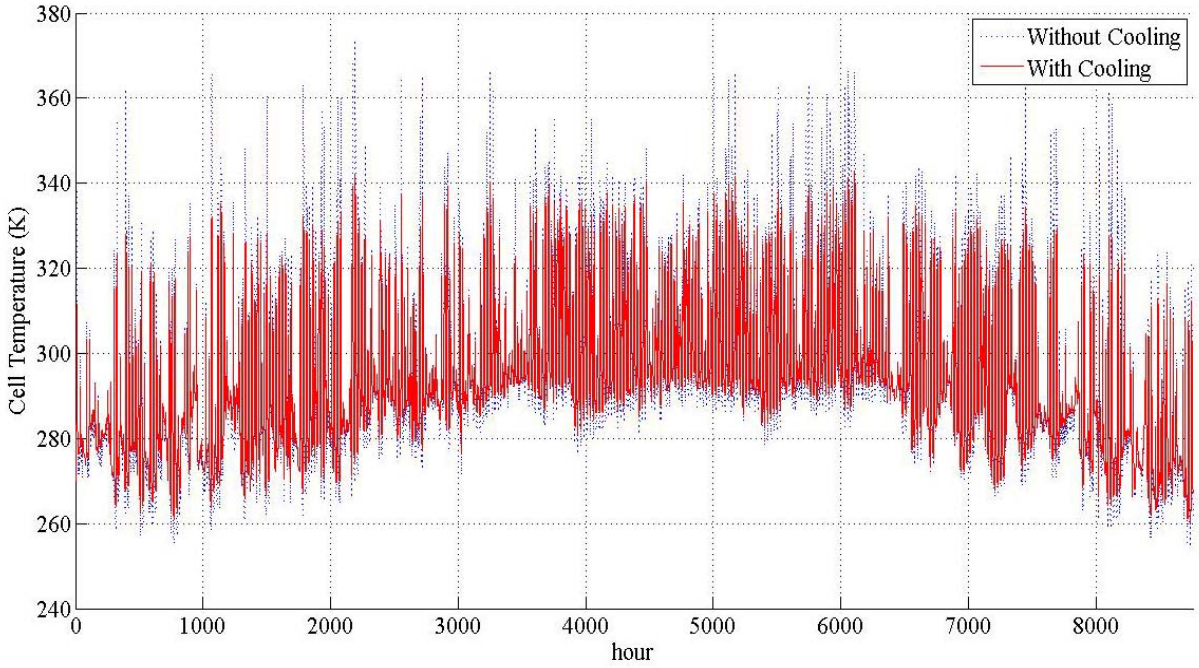

Figure 22: Cell temperature for systems with and without cooling

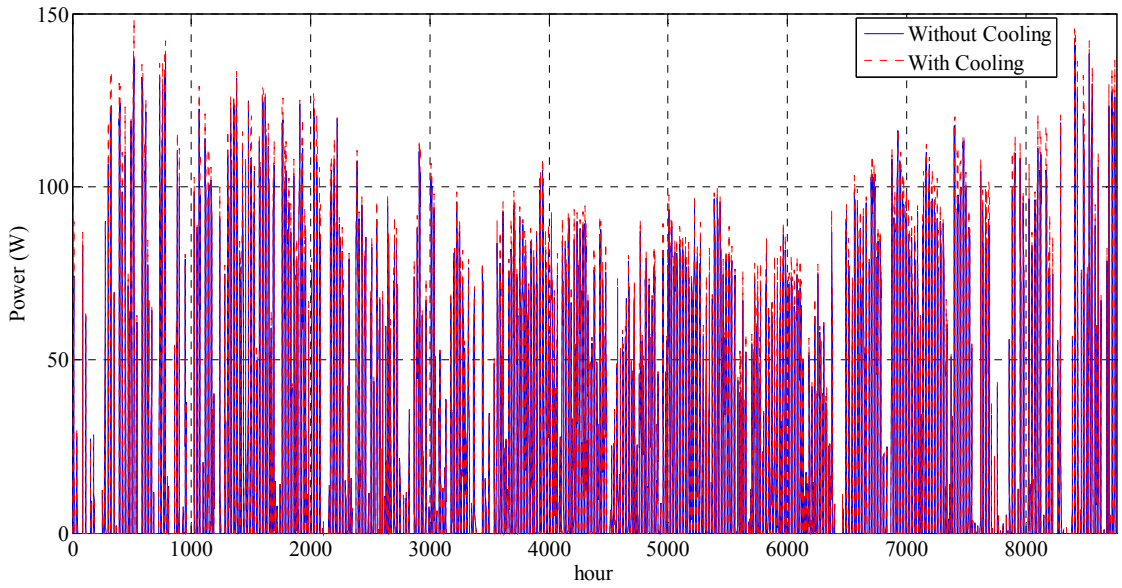

Figure 23: Comparison of the generated power by systems with and without cooling

It is also important to mention that the reason that this cooling approach does not seem to work very well during the hot season, is the air flow temperature is considered equal to the ambient temperature. Therefore, when the ambient temperature is high, the cooling effect of the air flow reduces. However, it can be seen that by using this cooling method, the cell temperature could be always kept well below the advised limit. It is obvious that by increasing the air flow through the air channel, more cooling effect will be provided for the solar panel. However, more air velocity needs more power to run the fans and a trade off needs to be made before select the appropriate air flow and fan devices.

CHAPTER 3: THERMOELECTRIC POWER GENERATION SYSTEMS

In this chapter, the use of thermoelectric power generator modules (TEG) to harvest the excess heat out of solar panels is investigated. The idea of converting temperature gradient to electricity is the main concept of using TEG modules. A mathematical model is developed and implemented in MATLAB to simulate the system performance under different conditions. The results are presented via several graphs showing the power generated and the efficiency of the system.

Thermoelectric Power Generation Modules (Seeback Effect)

The thermoelectric effect is the direct conversion of temperature differences to electric voltage and vice-versa. A thermoelectric device generates a voltage due to temperature difference between two sides (Seebeck effect). Applying temperature gradient causes charge carriers in the material to move from the hot side to the cold side. A thermoelectric device includes two dissimilar semiconductors, p- and n-type, connected electrically in series and thermally in parallel.

Thermoelectric power generator (TEG) modules can be used to convert heat energy to electricity based on the Seebeck Effect. This effect can be utilized to recover waste heat in different industrial applications. They basically work like heat engines but are less bulky, have no moving parts and are usually more expensive and less efficient.

A schematic of a TEG module is given in Figure 24**.** For a TEG module, the voltage generated is directly proportional to the number of n-p couples, the temperature difference

between the top and bottom sides of the TEG and the Seebeck coefficients of the materials. The Seebeck coefficient is a function of temperature and material properties..

Thermoelectric generators can be applied in a variety of situations for heat recovery. Usually, TEGs are used for small applications where heat engines (such as Stirling engines**)** would not be possible. The efficiency of TEG devices is usually around 5-10%. Figure of merit which usually denoted by *Z*, is the quantity used to characterize the performance of thermoelectric devices. The figure of merit can be found by:

$$Z = \frac{S_m{}^2}{R_m.K_m} \tag{33}$$

where S_m is the Seebeck coefficient, R_m is the electrical resistance and K_m is thermal conductivity of the thermoelectric module.

The efficiency of thermoelectric devices is defined as below:

$$\eta = \frac{T_h - T_c}{T_h} \frac{\sqrt{1+ZT}-1}{\sqrt{1+ZT}+\frac{T_c}{T_h}} \tag{34}$$

It is noteworthy that since the TEG modules are actually heat engines, their maximum efficiency follows Carnot rule.

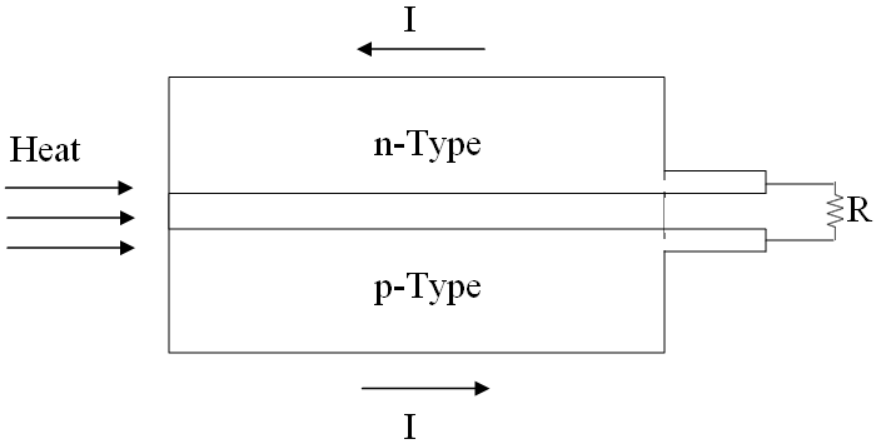

Figure 24: A schematic of a TEG module

As discussed in the first chapter, some researches investigated the use of TEG modules with solar energy systems. The idea of using TEG modules for harvesting excess heat from the PV panel is first proposed and discussed by Sark [30]. He considered installing TEG modules underneath PV cells and carried out an analysis to explore the performance of the system. The result from his work shows that using PV-TEG modules can potentially increase the annual energy yield by 11-14.7% for two annual irradiance and temperature profiles located in Malaga, Spain and Utrecht, Netherlands respectively. However, this work suffers from some inaccuracies owing to the over-simplified model which is used. Several heat losses have not considered including reflection losses. It is also assumed that the back side temperature of the TE converter always equals the ambient temperature which is not a very realistic assumption. An schematic from the system considered by Sark [30] is given in Figure 25.

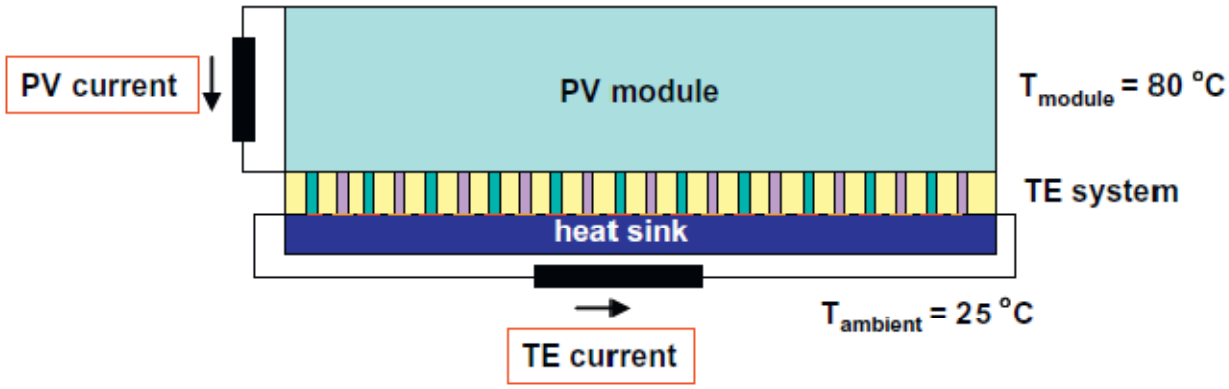

Figure 25: Schematic of the system considered by Sark [30]

In the present work, a comprehensive heat transfer model is developed in order to simulate the behavior of the combined PVT-TEG system. The temperature through different sections of the system is determined and the performance of the system under different irradiation levels is presented. The result of the simulation is presented via several graphs which shows how combined PVT-TEG system can increase the overall power generation and efficiency of the system.

Thermal Model for TEG

A schematic of the proposed system is shown in Figure 26. As can be seen, the TEG modules are installed in the back side of the PV panel.

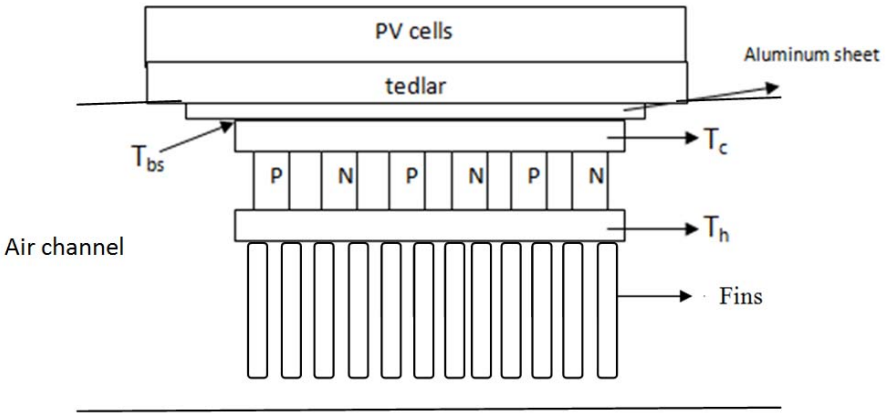

Figure 26: Schematic of combined PVT-TEG system

A portion of the heat removed from the PV panel (Q_h) through the TEG modules is converted to electricity and the majority of it will be rejected to the air through the fin surfaces in the air channel. The mathematical analysis of the system is explained in this section.

A schematic of a TEG module with fins installed on the back side of it is demonstrated in Figure 27.

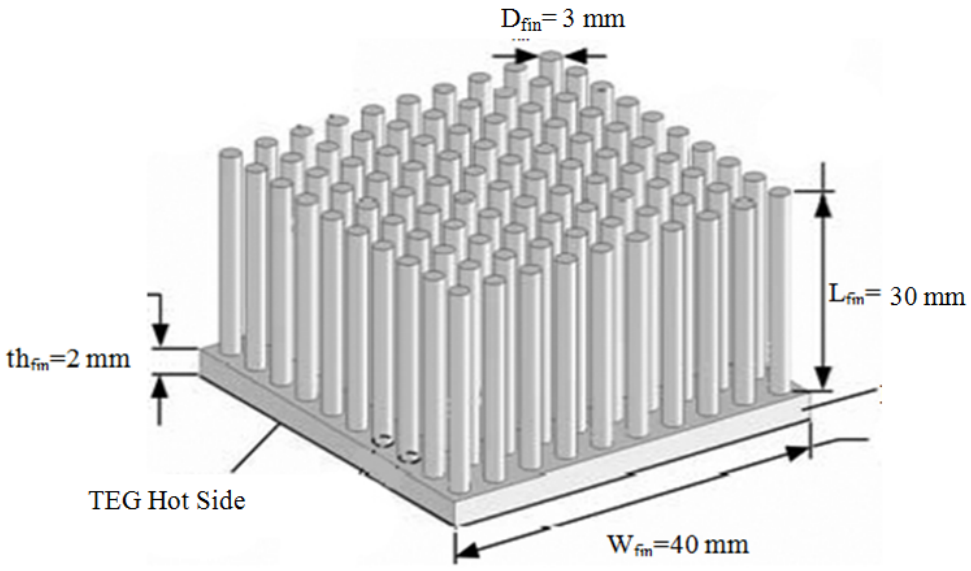

Figure 27: TEG module and cooling fins

The useful output power generated by the TEG module can be calculated by [9]:

$$P_g = S_m I_{teg}\left(T_h - T_c\right) - I_{teg}{}^2 R_m \tag{35}$$

where S_m is the Seebeck coefficient and R_m is electrical resistance of the TEG module, T_h is the temperature of the backside of the tedlar (T_h=T_{bs}), I_{teg} is the output current of the TEG module. In order to achieve the highest possible power, the optimal I_{teg} can be found as:

$$I_{teg} = \frac{S_m\left(T_h - T_c\right)}{2R_m} \tag{36}$$

The heat supplied to the hot side of the TEG from the tedlar can be found by conduction through the system as [22]:

$$Q_h = \frac{K_m A_m\left(T_h - T_c\right)}{t_m} \tag{37}$$

where A_m and t_m are the surface area and the thickness of the TEG module respectively. A small part of the heat supplied to the module converts to the power and the rest of it is rejected through the back side of the TEG module and the fins:

$$Q_h = Q_c + P_{teg} \tag{38}$$

The value of Q_c can be found by calculating the total thermal resistance from the backside of the TEG module to the ambient air. The total heat transfer includes the conduction through the base and convection through the fin itself and the un-finned lower surface of the base.

The resistance to conduction through the base can be given as:

$$R_{b,cond} = \frac{th_b}{k_b W_{teg}{}^2} \tag{39}$$

where k_b is the conductivity of the base and is equal to 25 W/mK. The resistance to convection through the fins can be found as [10]:

$$R_{fin} = \frac{1}{\eta_{fin} h A_{s,fin}} \tag{40}$$

where η_{fin} is the fin efficiency and can be expressed as:

$$\eta_{fin} = \frac{\tanh\left(mL_{fin}\right)}{mL_{fin}} \tag{41}$$

And m is the fin constant which is defined as [10]:

$$m = \sqrt{\frac{P_{fin} h}{k_{fin} L_{fin}}} \tag{42}$$

where P_{fin} is the fin perimeter. And finally the resistance of the un-finned surface of the base is calculated as:

$$R_{un-finned} = \frac{1}{h\left(W_b{}^2 - N_{fin} A_c\right)} \tag{43}$$

Therefore, the total thermal resistance is determined as:

$$R_{total} = R_b + \left[\frac{1}{\frac{R_{fin}}{N_{fin}}} + \frac{1}{R_{un-finned}} \right]^{-1} \quad (44)$$

Using the total thermal resistance between the backside (cold side) of the TEG module and the ambient air, the value of rejected heat (Qc) can be calculated as:

$$Q_c = \frac{T_c - T_a}{R_{total}} \quad (45)$$

Simulation and Results

The characteristics of the considered TEG module for simulation is given in Table 3 . is considered that an array with 100 pin fins is installed on the back side (cold side) of each TEG module. Each fin has the diameter of 3 mm and length of 30 mm. Considering the given geometry in Figure 27, the value of R_{tot} is calculated as 4.8 K/W. This value has a significant effect in the performance of the system. A lower thermal resistance leads to higher heat transfer and as a result higher temperature gradient between the two faces of the TEG module. This value subsequently used in the equations of combined PVT-TEG system to solve the system of equation which governs the system. The wind speed is considered as 2 m/s which flows through the fins and the backside of the PV panel.

Table 3: TEG module characteristics

Parameter	Value
S_{teg}	0.03 V/K
Z_{teg}	0.0024 1/K
Dimensions	40 x 40 x 4 mm
R_{teg}	1.18 Ω

For the first simulation, a single solar cell with the characteristics given in Table 4 is considered. It is considered that one TEG module is installed in the backside of the PV cell.

Table 4: PV cell characteristics

Short circuit current, I_{sc} (A)	4.65
Open circuit voltage, V_{oc} (V)	0.602
Maximum power current, V_{mp} (V)	0.479
Maximum power voltage, I_{mp} (A)	4.3
Short circuit current temperature coef. (A/K)	0.00372
Open circuit current voltage coef. (V/K)	-0.001986
NOCT, (C)	45
Dimension, (mm)	125×125×0.5
Efficiency, %	13

The following equations are required to be solved simultaneously to find the unknown parameters through the system.

The rate of solar energy available on PV module is equal to the sum of the overall heat loss from the top surface of PV cell to the ambient including radiative, convective and conductive losses, the overall heat transfer from the PV cell to the back surface of tedlar and the rate of electrical energy produced. This equilibrium is given in Eq. 1 which is shown here again [40]:

$$\tau_g \left[\alpha_c \beta_c G + \alpha_T (1-\beta_c) G \right] A_{PV} = U_t \left(T_{cell} - T_{amb} \right) A_{PV} + \varepsilon_g \sigma A_{PV} \left(T^4_{cell} - T^4_{sky} \right) + U_T \left(T_{cell} - T_{bs} \right) A_{PV} + \tau_g \beta_c \eta_{el} G \, A_{PV}$$

An energy balance equation can be also written for the back surface of tedlar:

$$U_T \left(T_{cell} - T_{bs} \right) A_{PV} = \mathrm{h}_a \left(T_{bs} - T_m \right) A_{PV} + \mathrm{P}_{teg} \mathrm{N}_{teg} \quad (46)$$

The first term in the right hand side refers to the heat removed by convection between the tedlar and the flowing air and the second term represents the generated power by the TEG modules.

These two equations (Equations 1 and 46), alongside equations 35, 36, 37, 38 and 45 are solved simultaneously in order to find the seven unknown parameters of the problem (T_{CELL}, T_{BS}, T_C, Q_H, Q_C, P_{TEG}, I_{TEG}) for specific ambient condition.

Figure 28 shows the variation of T_{cell}, T_{bs} (backside of tedlar) and T_c (cold side of TEG module) versus solar irradiance. As can be expected, the value of T_{cell} is always greater than T_{bs} and T_{bs} is greater than T_c. It is important that considering the upper temperature limit of the PV panel which is 85 C (358 K), for the current configuration, the solar irradiance should not exceed 2600 W/m^2 which is 2.6 suns and can be achieved by a low concentrating photovoltaic system in most areas. The temperature difference between T_{bs} and T_c is actually the gradient through the TEG module which causes power generation by the TEG module. The figure shows that higher solar irradiance leads to higher temperature difference through the TEG and consequently more output power. However, higher solar irradiance which could be achieved under concentration would cause higher cell temperature which necessitates using more effective and more expensive cooling methods.

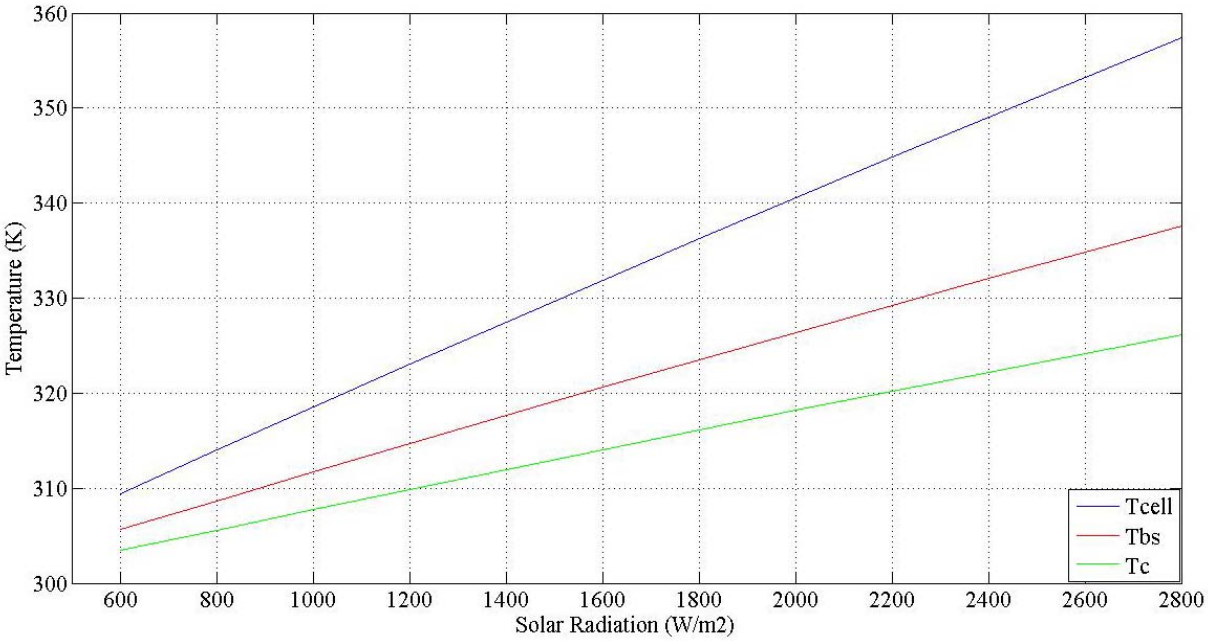

Figure 28: Variation of cell temperature, tedlar backside temperature and TEG's cold side temperature with solar irradiance

The variation of generated power via PV panel and the TEG module versus solar irradiation are given in Figure 29 and Figure 30 respectively. It can be seen that by increasing solar radiation the generated power would also increase. As can be seen, the panel produces 1.71 W at 1 sun irradiance (1000 W/m2), 3.12 W at 2 suns and 3.78 W at the maximum possible irradiation level for this configuration (2600 W/m2).

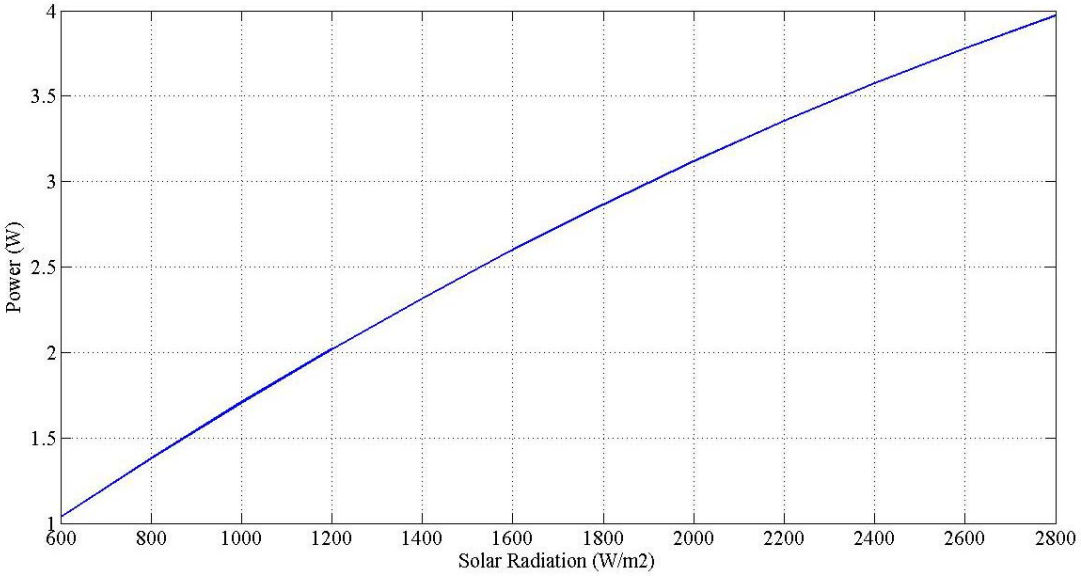

Figure 29: Generated power by PV

Figure 30 demonstrates the generated power by the TEG module. It can be seen that as the solar irradiance rises, the generated power increases with a growing rate. The solar irradiance varies from 600 to 2600 W/m^2 the generated power increases from 0.00643 W to 0.149 W.

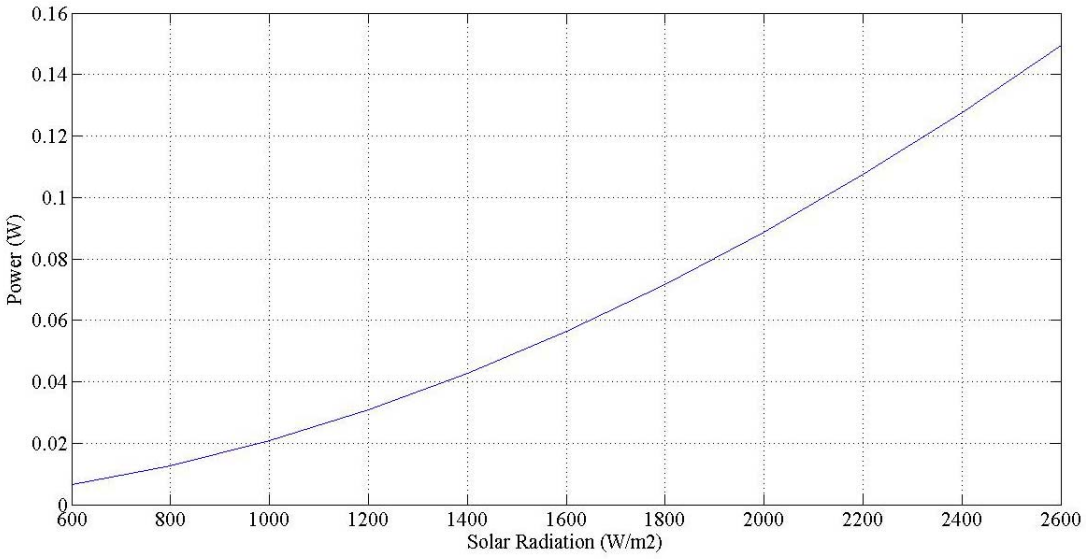

Figure 30: Generated power by TEG under different radiation level

Therefore, it could be inferred that, by installing one TEG module on a PV module and at the current conditions, the value of generated power by TEGs is about 0.0208, 0.0888 and 0.1494W under solar irradiance of 1, 2 and 2.6 suns. These values are about 1.21%, 2.84% and 3.95 % of the generated power by the PV panel at the same value for irradiation. However, this value could be increased by increasing the temperature gradient between the two surfaces of the TEG module. This can happen at higher concentration levels and by utilizing more efficient cooling methods for solar cells.

The variation of efficiency for the PV module and TEG module versus solar radiation is presented in Figure 31 and Figure 32. As can be seen the efficiency of the TEG module increases for higher solar radiation which is due to higher temperature gradient through the TEG module. The efficiency of the PV module would decrease due to temperature increment in the PV cell.

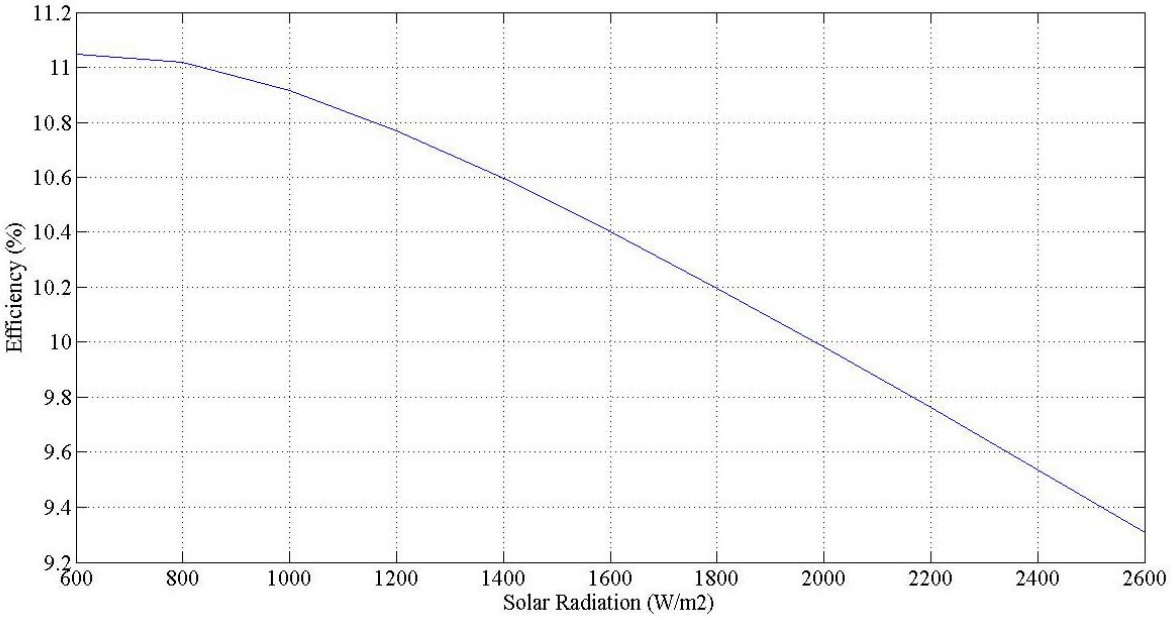

Figure 31: PV efficiency variation by solar radiation

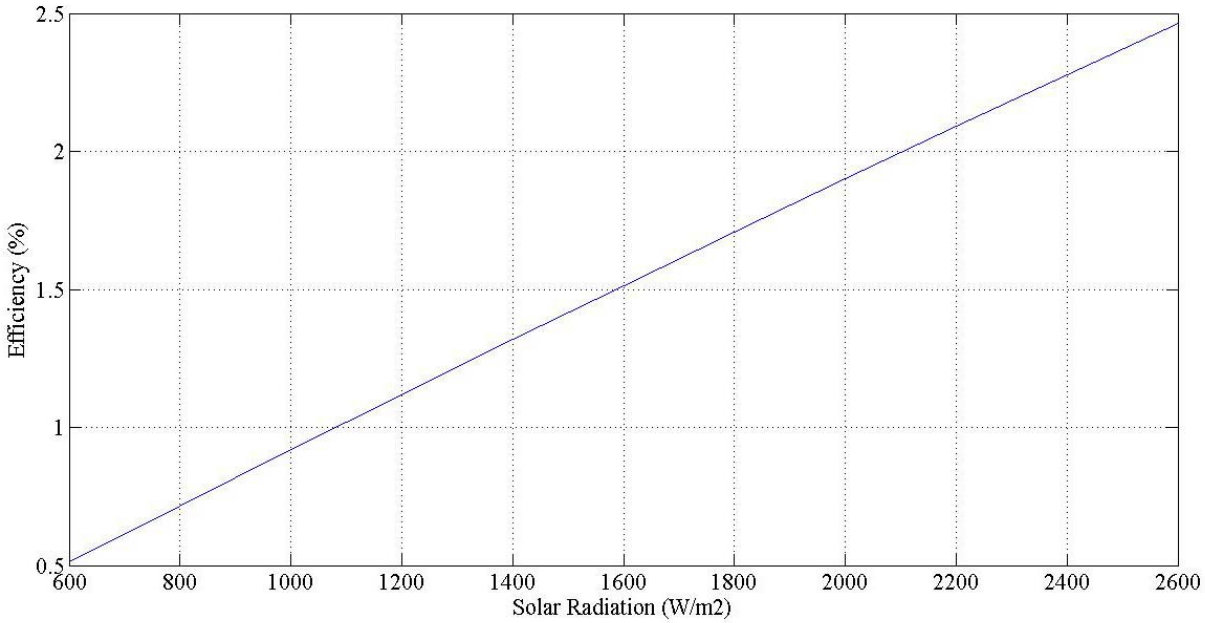

Figure 32: Variation of TEG module efficiency for different values of solar radiation

To explore the effect of the value of R_{tot}, which is the total heat resistivity of the heat sink, on the performance of the system the variation of temperature gradient versus R value under 2 suns (2000 W/m^2) solar radiation is investigated in Figure 33. It can be seen that a lower R can greatly increase the performance of the system. Therefore, a better heat sink can make a significant effect on the temperature gradient between two faces of the TEG module and as the result generating more power. The effect of R value on total generated power by the TEG module is depicted in Figure 34. It is shown that the produced power when R_{tot} varies between 10 and 0.5 would increase from 0.04 to 0.23 W which clearly shows the significant effect of the heat sink.

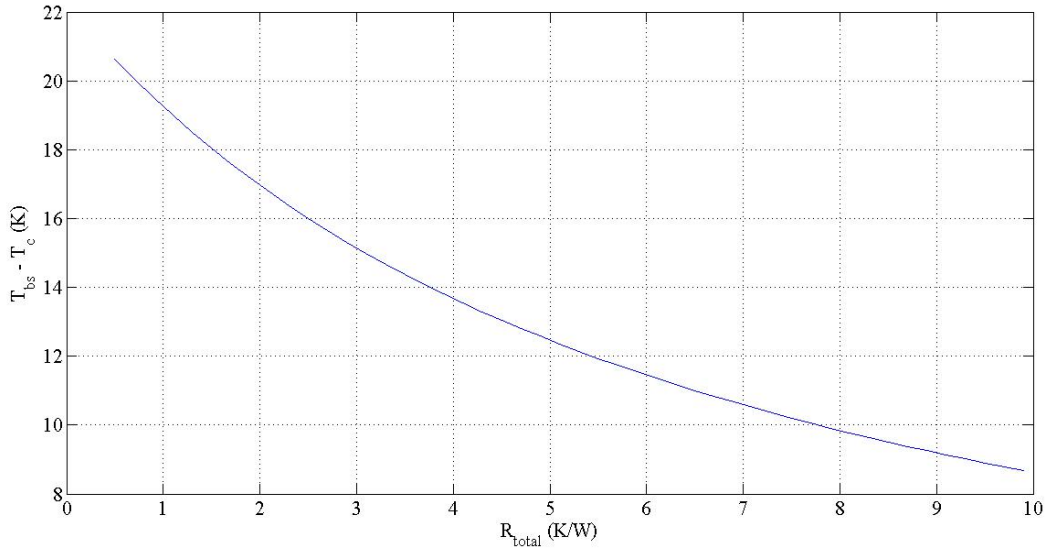

Figure 33: Effect of R on temperature gradient between two faces of the TEG module

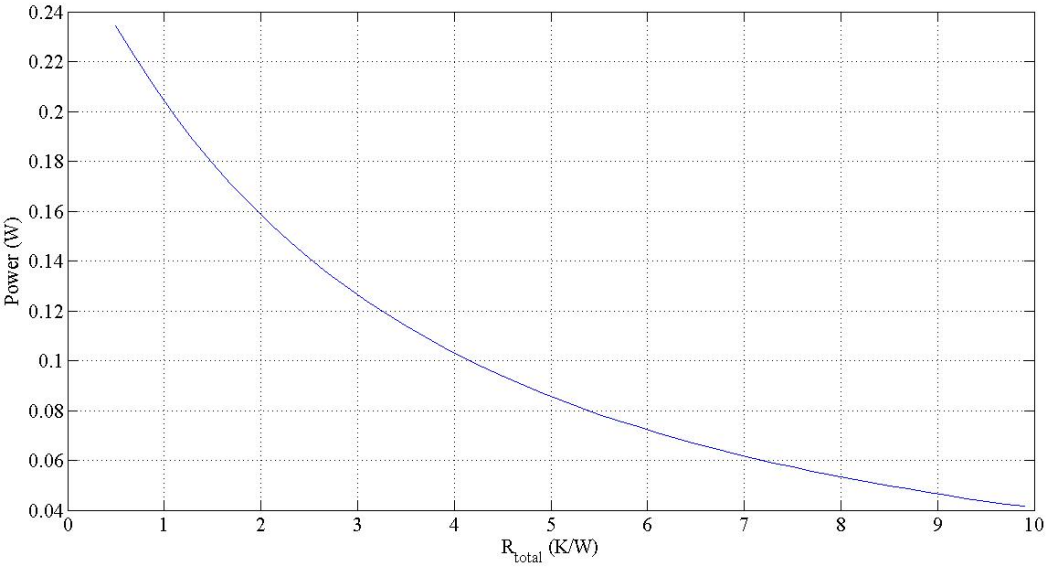

Figure 34: Variation of TEG generated power by thermal resistance (R)

The effect of ambient temperature on the system's performance is demonstrated in Figure 35 and Figure 36 while the solar radiation is still considered 2000 W/m2. Figure 35 shows how temperature gradient between the two faces of the TEG module varies with ambient temperature.

When the ambient temperature ranges from 280 K to 313 K and the generated power varies between 0.071 W and 0.105 W which is demonstrated in Figure 36.

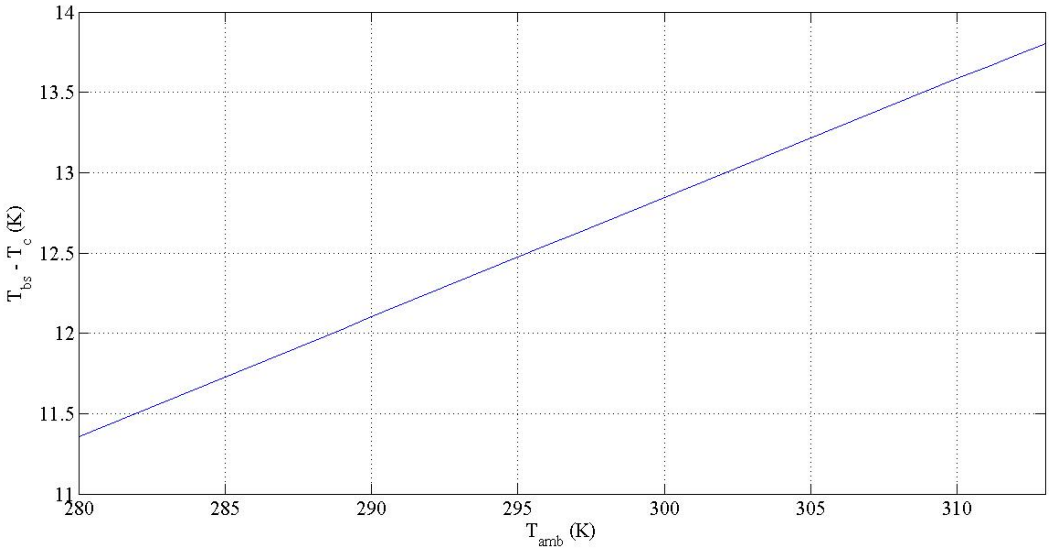

Figure 35: Ambient temperature effect on temperature gradient through the TEG module

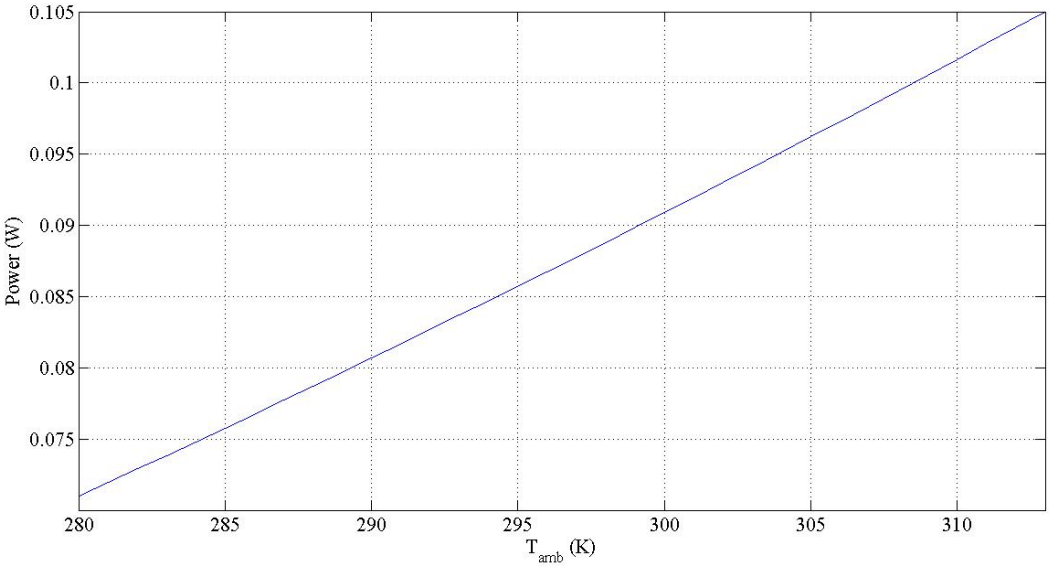

Figure 36: effect of ambient temperature on generated power by TEG module

Another simulation is carried out for a PV panel which includes 36 PV cells. The PV panel considered is the same panel which was considered in chapter 2 and the characteristics of this panel are given in Table 1. Thirty six TEG modules are installed in the backside of this panel inside an air channel which provides cooling effect for PV cells. So this time the simulation is performed on a larger scale.

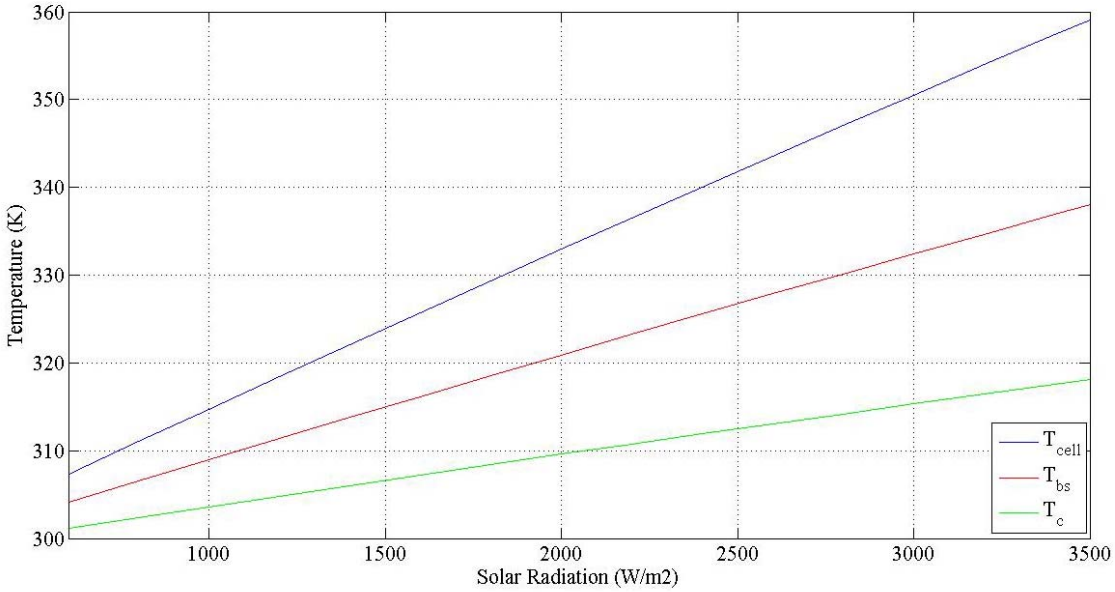

Figure 37: Temperature profiles for the combined TEG-PV system

Air is flowing with the speed of 3 m/s through the air channel to keep the solar panel at a lower temperature. By using the air flow for cooling, the radiation level could rise up to 3500 W/m^2. The temperature profile which shows cell temperature, backside temperature and cold side temperature of the TEG modules is shown in Figure 37. It should be noted that the value of convective heat transfer coefficient is determined via a similar procedure which is given in Chapter 2.

The power generated by the PV panel is given in Figure 38 as can be seen the power is varying from 46.7 to 192.8 W while the solar radiation varies from 600 to 3500 W/m^2. The power generated by 36 TEG modules is presented in Figure 39. The generated power by the TEG

modules is 0.579 W at 1 sun, 2.54 W at 2 suns, 5.78 W at 3 suns and 7.85 W at 3.5 suns. These values are about 0.75%, 1.83%, 3.22% and 4.07% of the total generated power by the PV panel. It is also possible to increase the number of TEG modules. Since the surface area of the PV panel is much larger than TEG modules it is possible to have two (or more) TEG modules per each PV cell. However, this might have some practical issues for installation and implementation. Moreover, the cost of each piece of TEG modules is about $23, so economic considerations must be taken into account before any decision is make.

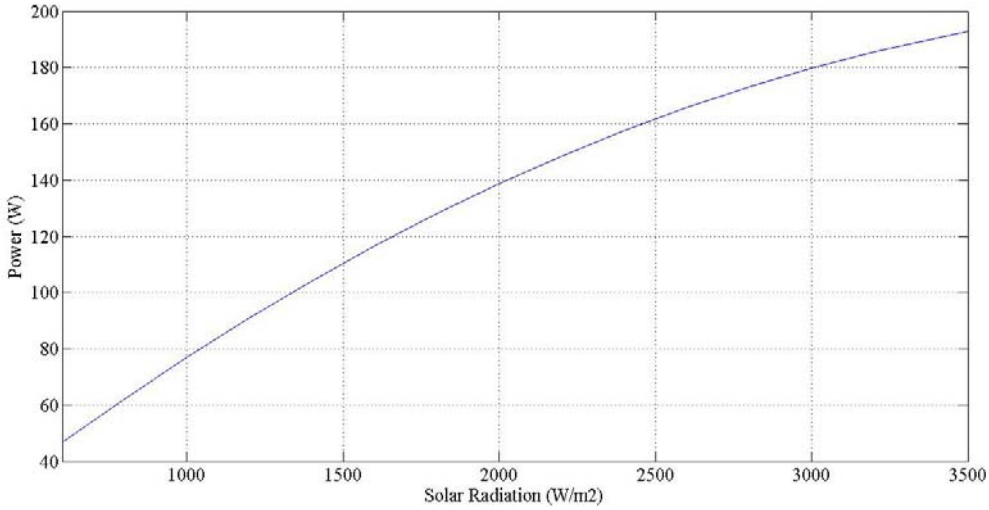

Figure 38: generated power by the PVT panel

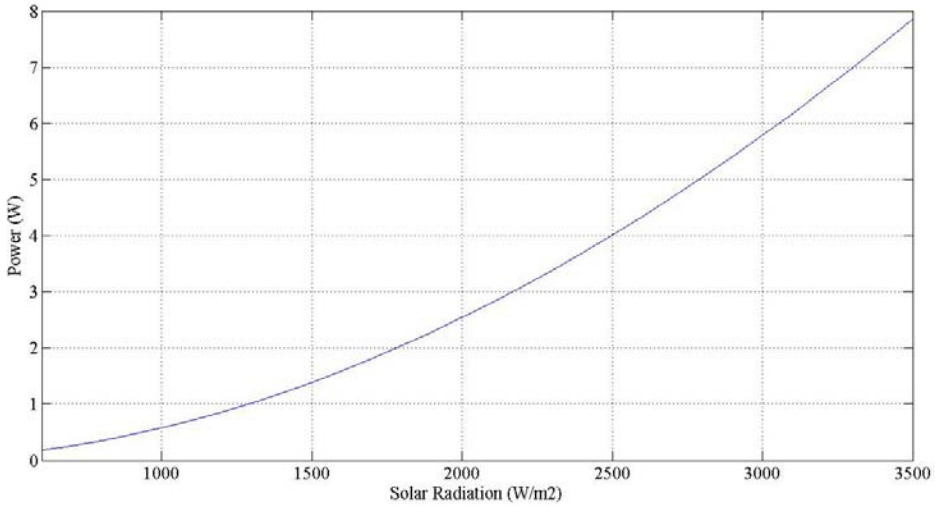

Figure 39: generated power by 36 TEG modules

The simulation shows that the TEG modules can add some amount of electricity to the total generated power by the PV panel. This value could become more significant at higher level concentrations and by using more effective cooling approaches. Therefore, it seems that in high concentration levels, using TEG could add considerable amount of power to the PV panel and could be an option to increase the total efficiency of the system.

A final simulation is performed to determine the daily and annual generated power by a combined PVT-TEG system in Tuscaloosa, Al. The same SP 75 solar panel is considered for the simulation. As shown in Figure 37, the cell temperature gets close to the limit (358 K) at solar radiation of 3500 W/m^2. It is assumed that the air flows through the channel with the speed of 3 m/s and at the ambient temperature. All the weather data are obtained from TMY3 data base. Considering the ambient conditions in Tuscaloosa, AL, including the solar radiation level, wind speed and the ambient temperature, a 3x concentration level will be achievable for the system without exceeding the temperature limit for the considered panel.

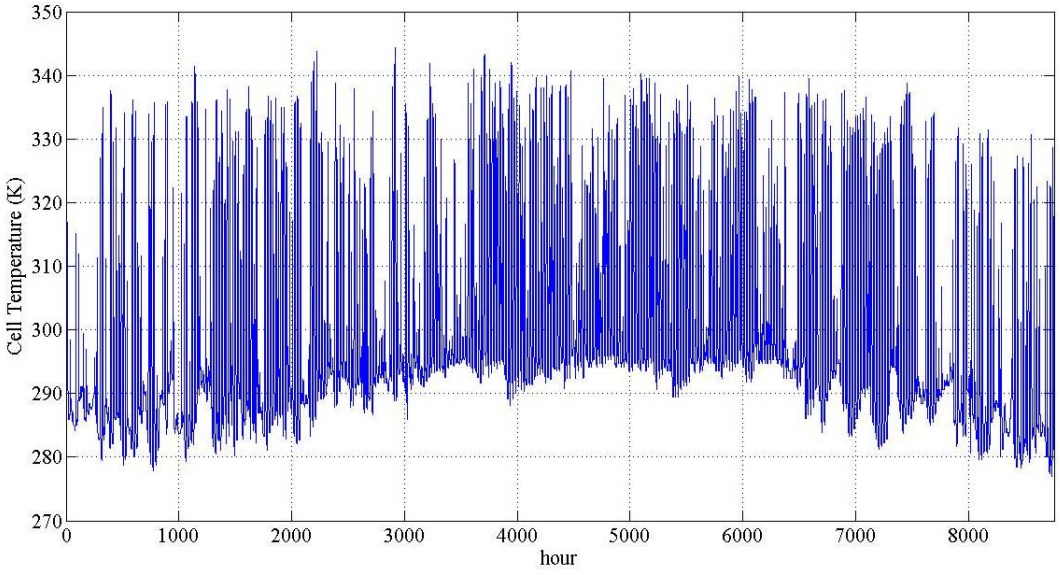

Figure 40: Annual temperature profile for combined PV-TEG system

Figure 40 shows the temperature profile during a year under considered conditions. It can be seen that the temperature does not exceed the defined range (358 K) and the PV panel can work appropriately.

The simulation is first performed for a specific day (July 29th). The collectible direct solar radiation profile and the ambient temperature profile are given in Figure 41 and Figure 42.

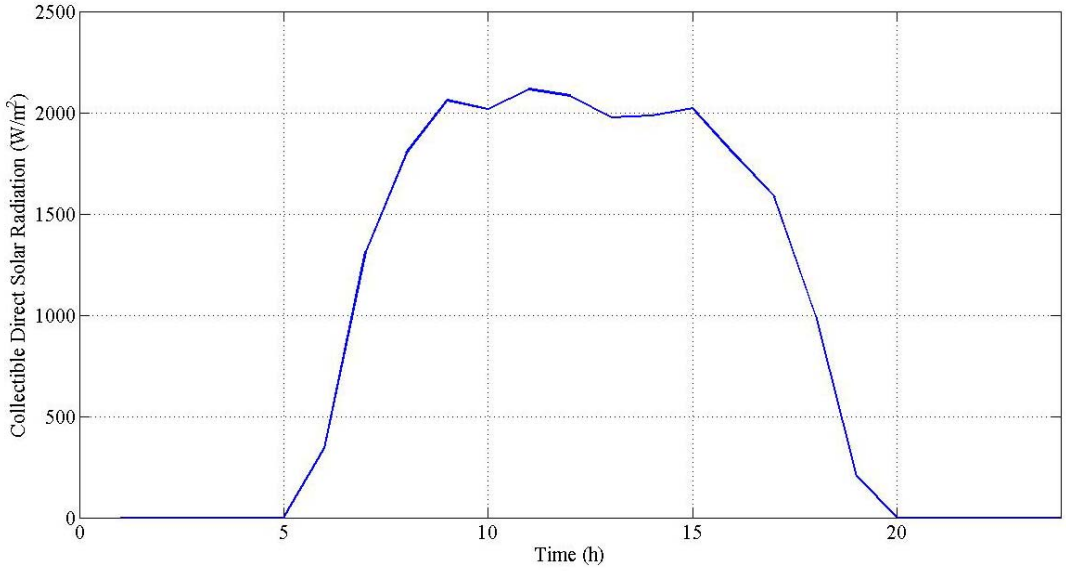

Figure 41: Collectible direct solar radiation on July 29th

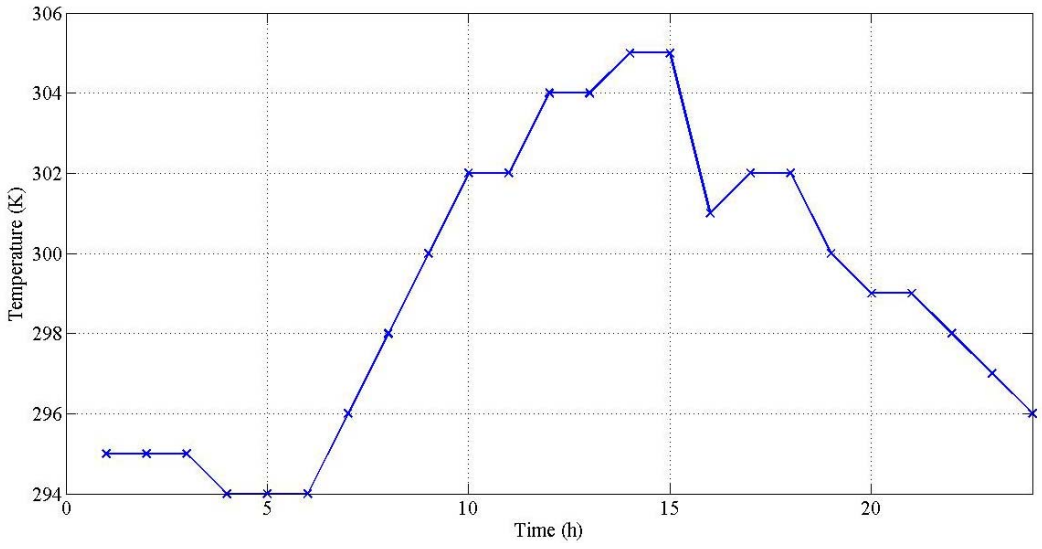

Figure 42: Ambient temperature profile for July 29th

The generated power by the PV and TEG modules are shown in Figure 43 and Figure 44 respectively.

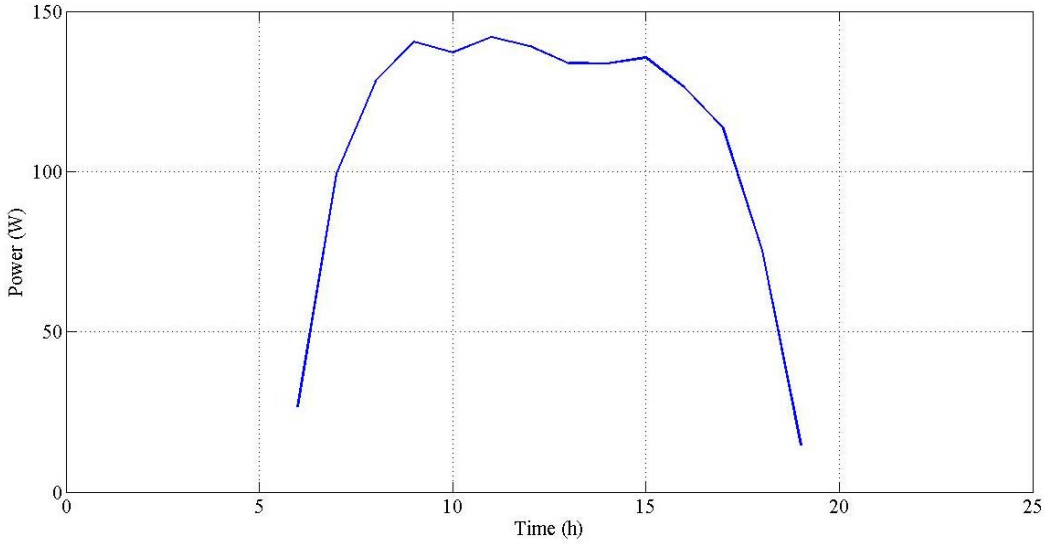

Figure 43: Generated power by the PV panel

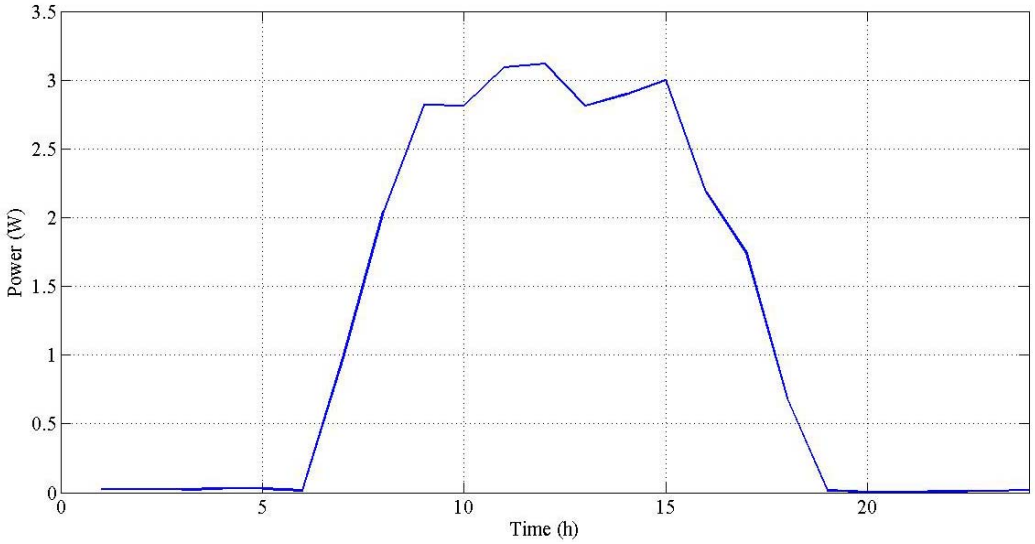

Figure 44: Generated power by the TEG module

As can be seen, when the solar radiation is higher, which occurs around noon, the output of both PV and TEG modules increases significantly. The total generated electricity by TEG

modules during this day is 28.398 Wh which is 1.84% of the total generated electricity by the PV panel during the same time (1.54 kWh).

Finally, from the yearly simulation, the generated power via PV panel is depicted in Figure 45. The total generated electricity by the PV panel through the whole year is calculated as 263.9 kWh. It should be noted that since the finned plates are installed in the back side of the TEG modules, they really helped the cooling process through the air channel and allows slightly higher concentration levels for the same air flow.

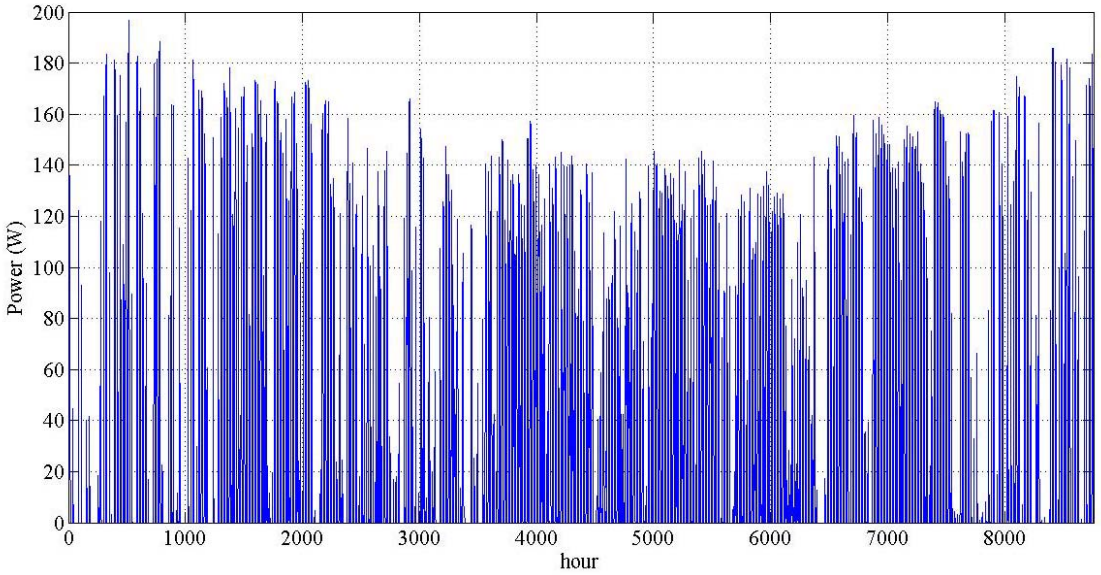

Figure 45: Generated power by PV panel

The generated power by TEG modules is demonstrated in Figure 46. The total generated electricity during the whole year is 4.32 kWh which is 1.64 % of the total generated power by the PV panel. Although this value is obviously not remarkable, it could be improved by using more efficient thermoelectric modules and probably higher concentration levels and more effective

cooling methods which can provide higher temperature gradient between two faces of the TEG modules.

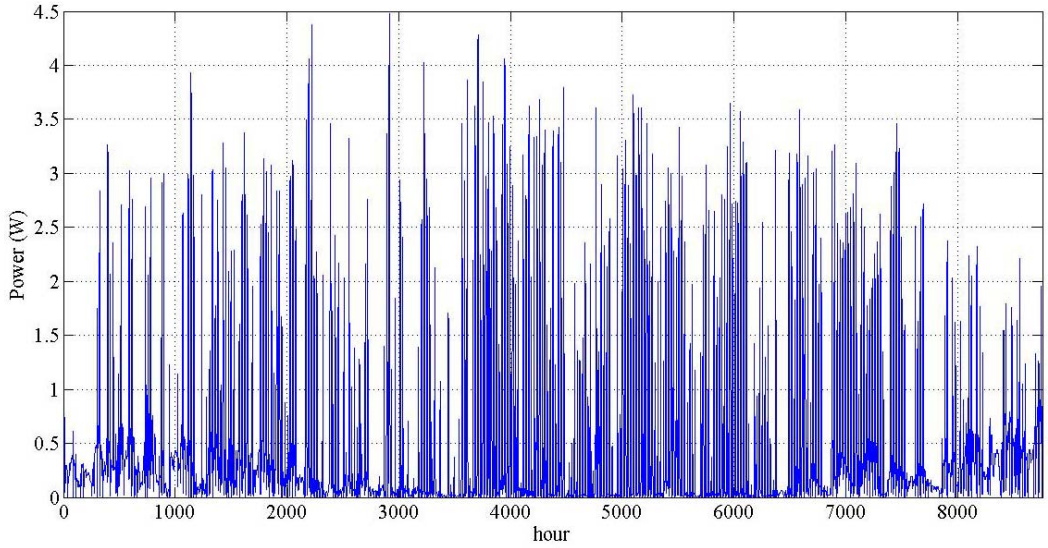

Figure 46: Generated power by TEG modules

CHAPTER 4: THERMOELECTRIC COOLING

In this chapter, the potential of using thermoelectric cooling modules (TEC) for temperature control of PV cells is investigated. A model is developed and implemented via MATLAB to predict the behavior of the combined PV-TEC system under different levels of solar radiation. An optimization procedure is also carried out via Genetic Algorithm (GA) method in order to find the optimal value of the supplied electric current to the TEC module which leads to highest output power.

Thermoelectric Cooling Modules (TEC)

A thermoelectric cooler (TEC) is a semiconductor-based electronic component that works similar to a small heat pump. This device made of two dissimilar semiconductors, p- and n-type, connected electrically in series and thermally in parallel. A schematic of TEC module is shown in Figure 47. These thermoelectric element and their electrical interconnects typically are mounted between two ceramic substrates. The substrates serve to mechanically hold the overall structure together and to electrically insulate the individual elements from one another and from external mounting surfaces. By supplying a low-voltage from a DC power source to a TEC module, heat will be transferred from one side to another one. Consequently, one module face will be cooled while the opposite face simultaneously is heated.

The cooling with TEC modules can be compared with cooling in a typical mechanical refrigeration unit. In a mechanical refrigeration unit, a compressor raises the pressure of the refrigerant, compresses the gas which is then cooled into a liquid, and circulates the refrigerant through the system. The refrigerant evaporates in evaporator by absorbing heat and goes to the condenser where the heat is rejected to the environment. In a thermoelectric cooling system

(TEC), a doped semiconductor material is used as the refrigerant, a finned heat sink represents the condenser and the compressor is replaced by a DC power source. Applying DC power to the TEC module causes electrons to move through the semiconductor material. At the cold face of the TEC module, heat is absorbed by the electron movement, moved through the material, and rejected at the hot face. The hot end of the material then rejects heat to the room air. The heat removed is proportional to the magnitude of the applied DC electrical current. By varying the input current from zero, it is possible to control the heat flow and temperature.

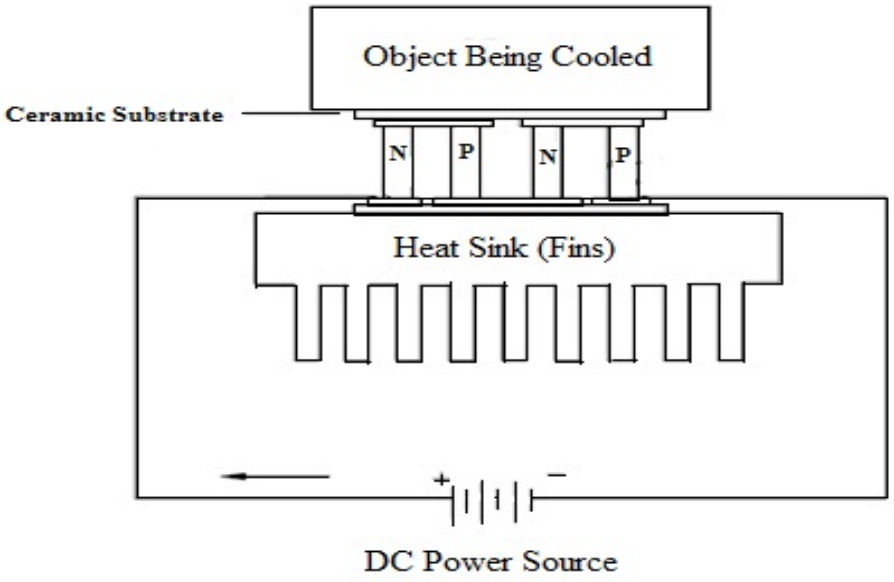

Figure 47: Schematic of TEC module

By using a heat sink, a thermoelectric cooler can lower the temperature of an object below ambient and stabilize the temperature of objects under different ambient conditions. A thermoelectric cooler is an active cooling device whereas a heat sink provides only passive cooling.

Thermoelectric coolers generally may be considered for applications that require heat removal ranging from milli watts up to several hundred watts. Most single-stage TE coolers,

including both high and low current devices, are capable of pumping a maximum of 3 to 6 watts per square centimeter (20 to 40 watts per square inch) of module surface area [51].

Small size and weight, ability to cool below ambient, ability to heat and cool with the same device, precise temperature control (up to ± 0.1°C), quiet and environmentally friendly operation, high reliability and ability for spot cooling are some of the main advantages of using TEC modules for cooling [51].

Combined PV-TEC System

The idea of combined PV-TEC system is a potential approach to provide a quiet and easy way for controlling the temperature on PV cells. As has discussed already, increasing the temperature can cause significant damages to the solar cells as well as losses in efficiency. Due to the varying nature of solar radiation, the allowable temperature range is a vital factor which needs to be considered before designing a PV system for a specific application. This is even more important on concentrating photovoltaic systems (CPV) systems when solar radiation could be much higher leading to higher cell temperature. Although there are several different ways to provide the cooling effect for solar cells, including active and passive methods, the importance of this task has encouraged more researchers to explore different new methods.

Active cooling methods are proved to be more effective specially for higher concentration level systems. The most common active cooling systems are based on using photovoltaic-thermal solar collectors (PVTs) which were explained, simulated and discussed in Chapter 2. Although this method has been maturing and nowadays is a rather cost-effective way to implement in several applications, it has some disadvantages which makes it inappropriate for

some other applications. Using PVT systems necessitates installation of pumping, plumbing or duct channels on the system which makes it massive and noisy. The temperature of the air/water which is used as the cooling fluid is usually equal to or very close to the ambient temperature which means that during the hottest hours the cooling effect would be literally the least. The controllability of temperature cannot be performed accurately, therefore, an oversized pump or fan might be used to provide cooling in order to prevent cell damage during few extremely hot hours during a year. The leakage is almost an inevitable problem in every plumbing system which increases the maintenance cost. Finally, for small applications, it is not possible to use PVT systems. It is important to note that in small applications, the temperature control is very important since the surface area is very limited and the heat transfer through it is small. Therefore, in order to avoid cell damage it is desirable to have some alternative cooling method which would be activated whenever temperature exceeds some specific recommended value.

Thermoelectric cooling modules are light, quiet and need least maintenance costs. They are also very small and it is possible to install them almost for any small application. The TEC modules operate using electricity and provide a temperature gradient between the two faces. Therefore, it is easy to control them by varying the electrical current and get desired amount of cooling effect regarding the application. Therefore, it seems that it is possible to use TEC modules to have some temperature control on solar cells. The power utilized by the TEC modules can be provided by the PV cell itself which makes the whole system more compact. However, care needs to be given about how much power is required to provide enough cooling effect for the solar cell.

In this chapter, an analysis is conducted on combined PV-TEC systems in order to evaluate the performance of the cooling effect provided by TEC modules on PV cells to, a)

enhance total output power due to temperature reduction, and b) to control the temperature for specific applications.

The optimization is performed by the Genetic Algorithm (GA) via a series of functions which is developed in MATLAB.

Thermal Model for TEC

TEC modules are most commonly specified by four main characteristics by vendors including I_{max}, V_{max}, Q_{max} and ΔT_{max}. The ΔT_{max} is the maximum temperature difference obtainable between the hot and the cold TEC sides at a given hot side temperature T_h, I_{max} is the input current that can produce the maximum ΔT_{max} across a TEC module, V_{max} is the DC voltage at the temperature difference of ΔT_{max} at $I = I_{max}$, and Q_{max} is the maximum amount of heat absorbed at the TEC cold side at $I = I_{max}$ and $\Delta T_{max} = 0$ [12].

Knowing these four values, the module parameters can be calculated as below [52]:

$$S_m = \frac{V_{\max}}{T_a} \tag{47}$$

$$R_m = \frac{(T_a - \Delta T_{\max})V_{\max}}{T_a I_{\max}} \tag{48}$$

$$K_m = \frac{(T_a - \Delta T_{\max})V_{\max} I_{\max}}{2T_a \Delta T_{\max}} \tag{49}$$

A schematic of a TEC module and thermal flows is depicted in Figure 48. *Rjc* and *Rha* in this figure represent junction to TEC thermal resistance and TEC hot side to ambient thermal resistance respectively.

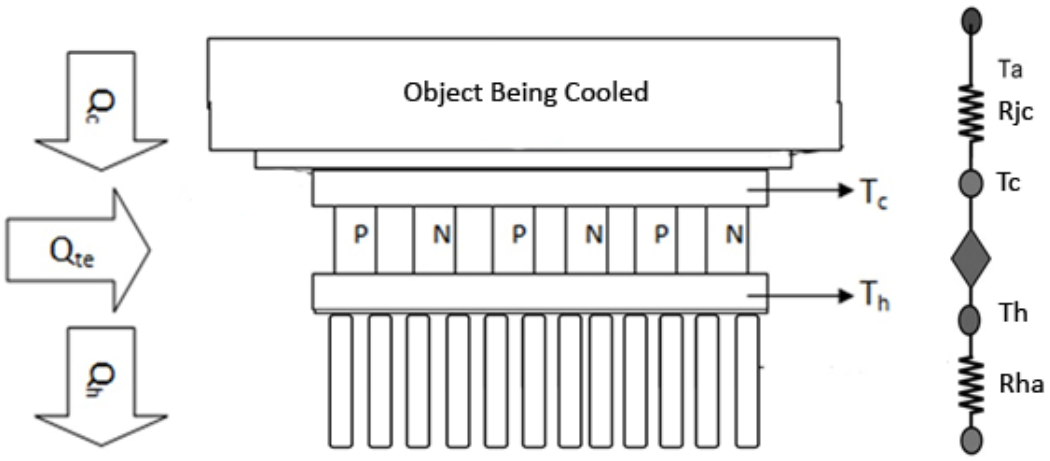

Figure 48: Schematic a TEC module and heat flows

From the thermal balance for a TEC module, the cooling power absorbed at the cold side can be found by [12]:

$$Q_c = S_m I_c T_c - \frac{I^2 R_m}{2} - K_m \Delta T \quad (50)$$

The generated heat at the hot side of TEC module can be calculated as:

$$Q_h = S_m I_c T_h + \frac{I_c^2 R_m}{2} - K_m \Delta T \quad (51)$$

where ΔT refers to the temperature difference between the hot side and the cold side of the TEC module:

$$\Delta T = T_h - T_c \quad (52)$$

The temperature at the junction between the backside of the PV panel (tedlar) and the Aluminum plate can be determined as:

$$T_{bs} = T_c + Q_c R_{jc} \quad (53)$$

The temperature at the hot side of the TEC can be found by:

$$T_h = T_a + Q_h R_{ha} \tag{54}$$

Finally, the energy conservation for the TEC module can be written as:

$$Q_h = Q_c + Q_{te} \tag{55}$$

In order to validate the model, a comparison between the results generated by this model and the results given in [52] is presented here. The variables given in Table 5:

Table 5: TEC parameters

Parameter	Value
I_{max}	19 A
Q_{max}	330 W
V_{max}	32 V
ΔT_{max}	64.5 K
T_{amb}	298K
R_{ha}	0.05 K/W
R_{jc}	0.267 K/W
$T_{amb,}\ T_j$	298 K
Dimensions	50×50 MM

At this point, the same conditions as were considered in the paper [52] and the results can be compared with the results presented in Zhang's paper. In Figure 49, the variation of temperature difference versus supplied electrical current to the TEC module for a constant value of cooling capacity (50W) is given. The left side shows the result from the Zhang's paper and the right side is the plot generated by MATLAB. It should be noted that the plot in the right side is corresponding to the top curve in the left graph. The asterisk shows the values of corresponding graph from Zhang [52].

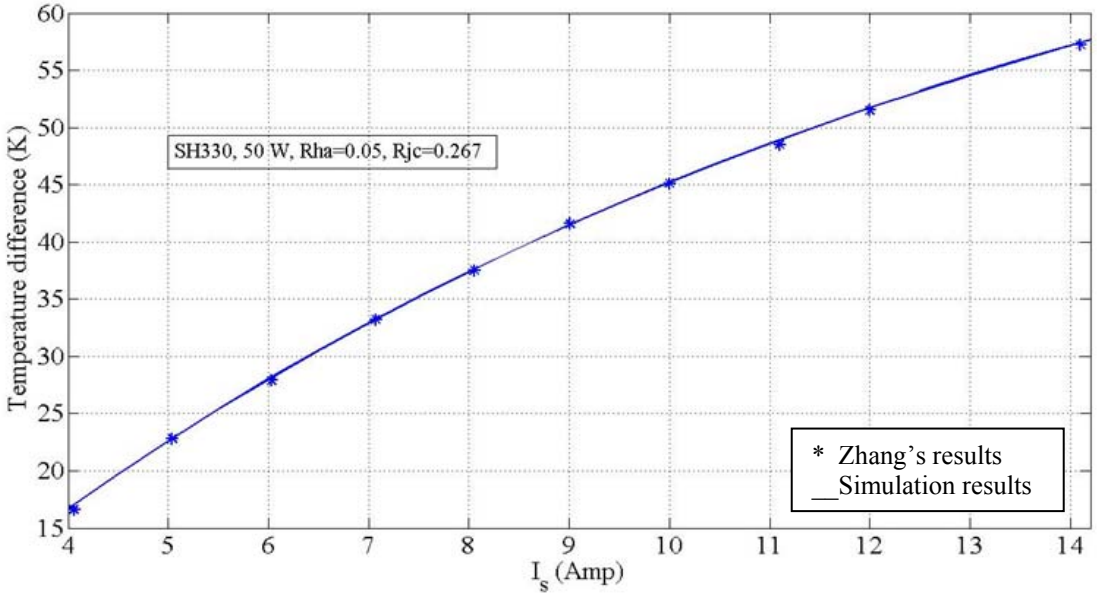

Figure 49: Results comparison with the results from Zhang [53]

In Figure 50, the variation of Q_c (heat removed by the TEC module) versus the supplied electrical current is demonstrated. Similarly, the conditions for the top curve in the left graph is used to generate the right plot. As can be seen, there is a very good agreement between the graphs.

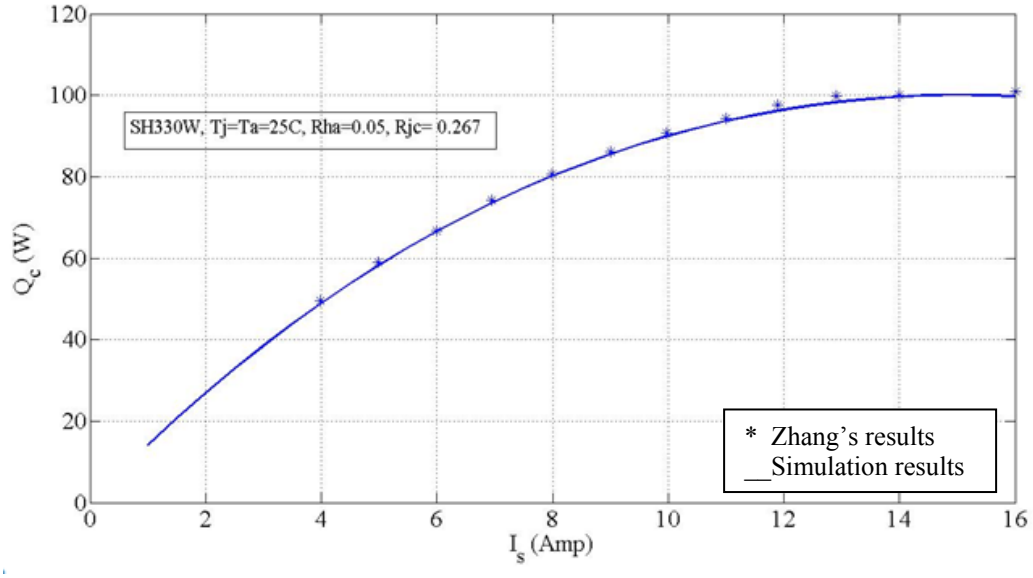

Figure 50: Results comparison with results from Zhang [53]

Genetic Algorithm

Genetic algorithm (GA) is a stochastic numerical search method, inspired by evolutionary processes, which was first conceived by Holland [53]. A comprehensive discussion about GA can be found in [53] and [54]. In GA terminology, a solution vector $x \in X$ is called an individual or a chromosome. GA operates with a collection of chromosomes called population. Chromosomes are made of discrete units called genes. Each gene controls one or more features of the chromosome [55]. The initial population is usually randomly generated. Afterwards, parents are selected based on their fitness values. The higher fitness of an individual, leads to higher possibility of being selected as parent for the reproduction. There are several methods for selecting the highly fitted parents and the roulette wheel method, which is probably the most common selection method, is used in this work. In this method a portion of the wheel is assign to each possible selection according to the fitness values. By dividing the fitness of each specific selection by the total fitness for all selections and normalizing to 1, the proportion of each selection on the roulette wheel can be evaluated. A random selection is then made similar to the roulette wheel rotation and the selections with higher proportions on the wheel have higher chance of being selected. In the next step, reproduction, two chromosomes (parents), combine together and form new chromosomes, called offspring. Since individuals with higher fitness have more chance for being selected and produce offspring, the new population, generated after reproduction, posses more qualified genes and consequently higher fitness. Therefore, using crossover operator iteratively leads to convergence to a general good solution. The mutation operator, which is generally applied in the genes level, causes random changes in characteristics of chromosomes. Since the mutation rate is small and depends on length of the chromosome, the new chromosome produced by mutation will not be much different from the earlier one. Hence,

crossover leads the population to converge by making the chromosomes in the population alike. Mutation reintroduces genetic diversity back into the population and assists the search to escape from local optima [55].

A set of functions are coded in MATLAB in order to perform the GA optimization procedure. The flowchart given in Figure 51 shows how GA works and converges to the optimal result.

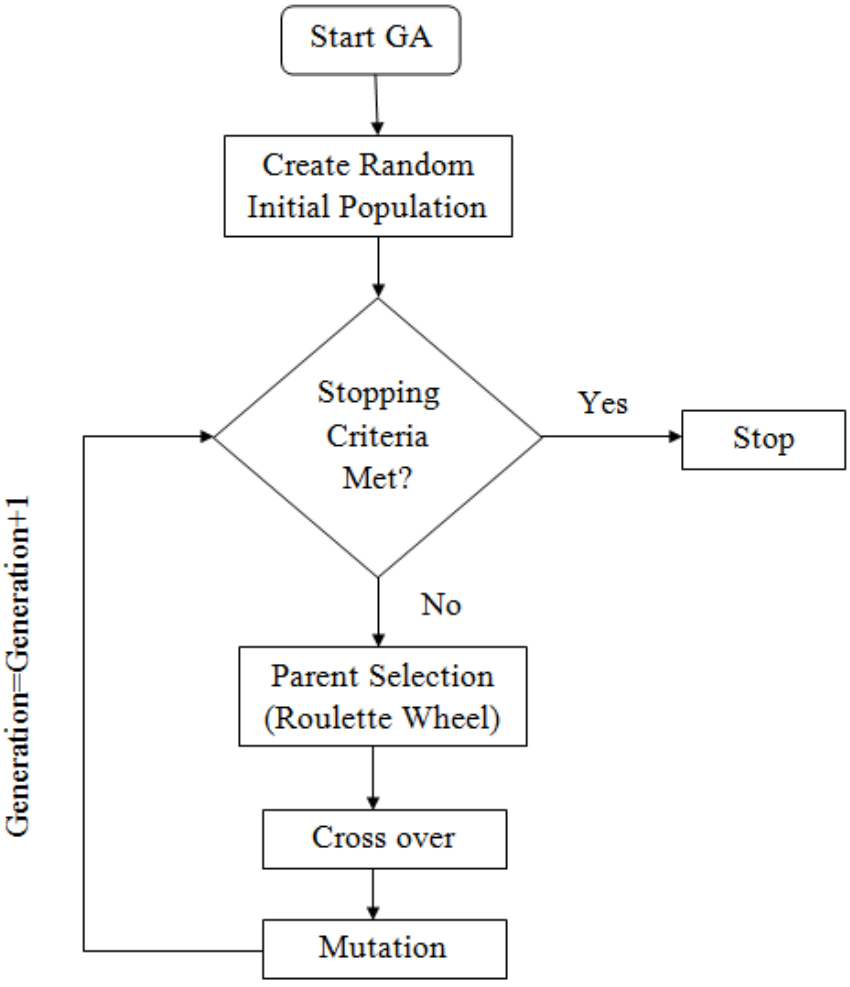

Figure 51: GA optimization flowchart

The considered values for GA optimization are given in the table below:

Table 6: Parameters used in Genetic Algorithm optimization

Parameter	Value
Chromosome	electrical current
No. of generations	30
Population size	25
Cross Over Probability	1
Mutation Probability	0.01

It should be noted that the stopping criteria in this work is defined as the number of generations.

Simulation and Results

A schematic of a TEC module installed in the back side of the PV panel is demonstrated in Figure 52.

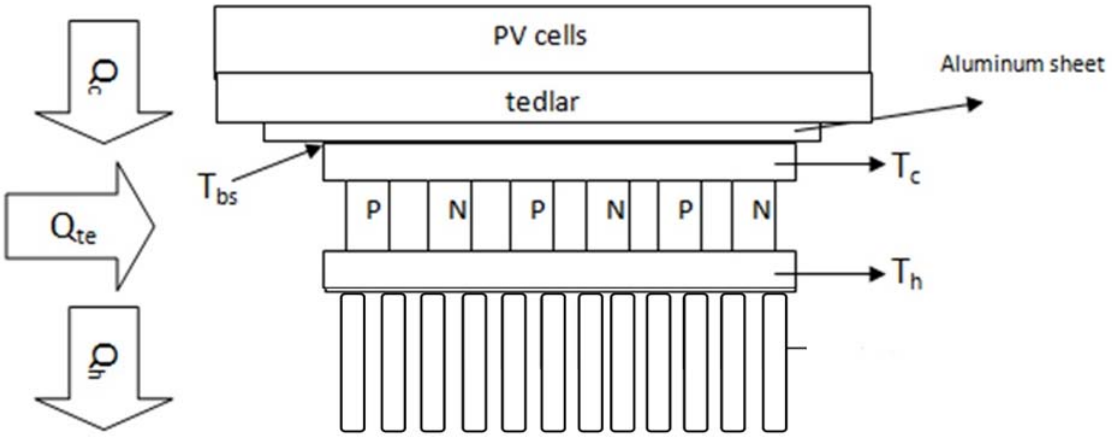

Figure 52: Schematic of the combined PV-TEC system

As can be seen in the figure above, TEC modules are considered to be installed in the back side of a PV cell. The characteristics of the PV cell and the considered TEC module are given in Table 4 and Table 7 respectively.

Table 7: TEC module characteristics (Marlow DT 12-401)

Parameter	Value
I_{max}	3.7 A
V_{max}	14.7 V
Q_{max}	36 W
ΔT_{max}	66
Dimensions	34×30×3.4 mm

The TEC module is supplied with electrical current generated by the PV cell. The magnitude of this current could be adjusted by the user.

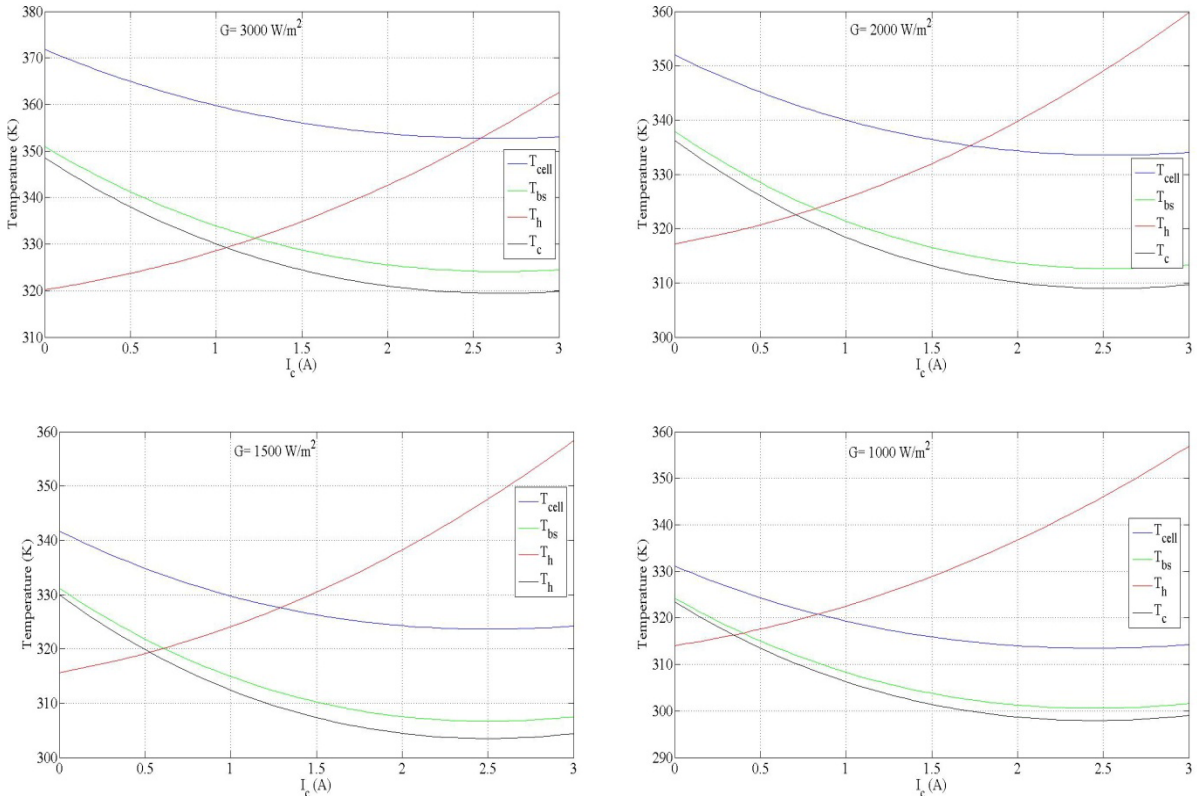

Figure 53: Temperature within the combined PV-TEC system

The variation of temperature at different sections of the system versus the supplied current to the TEC module for different values of solar radiation and at ambient temperature of 311 K is presented in Figure 53. The *Z* value (figure of merit) of the considered module is 0.0022 which is a typical value for TEC modules. As expected, increasing I_c results in more cooling effect which decreases cell temperature and tedlar backside temperature. However, increasing the I_c means supplying more power in to the TEC module. The utilized power by the TEC module can be given by following equation:

$$P_{TEC} = S_m I_c \left(T_h - T_c\right) + {I_c}^2 R_c \tag{56}$$

Figure 54 demonstrates the consumed power by the TEC for different values of I_c. For a specific set of conditions, it is possible to calculate the optimal value for electrical current which should be supplied to the TEC module in order to obtain the minimum junction temperature and

consequently minimum cell temperature. This approach is usually utilized for designing and optimization of refrigerators which work by TEC modules when maximizing the cooling effect is the main concern in the problem. However, this is not a feasible approach for PV-TEC systems since the required power to run the TEC at the optimal performance is way more than the power generated by PV cell.

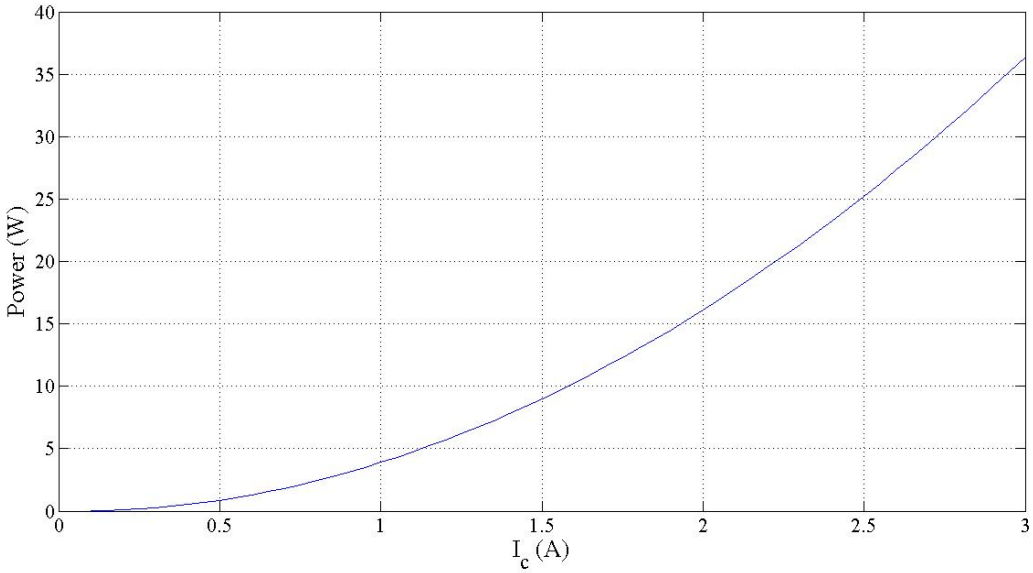

Figure 54: Power used by TEC module for different electrical current

To demonstrate this, a simulation is carried out in order to find the optimal required current for TEC modules and the results are given in Table 8. Therefore, it can be seen that although the TEC modules are capable of providing significant amount of cooling for PV cells, they use high amount of power which is more than the maximum generated power by PV modules.

Table 8: Optimal values of I_c which yields minimum T_{cell}

G (W/m2)	$Tcell_{, non\text{-}cooled}$ (K)	$Tcell_{, cooled}$ (K)	$I_{c,opt}$ (A)	PTEC (W)	$PPV_{, cooled}$ (W)
1000	329.6	313.5	2.33	23.25	1.72
2000	350.5	333.6	2.4	23.3	3.0896
2500	360.5	343.3	2.46	23.83	3.59
3000	369.6	352.9	2.55	25.39	3.98

Temperature Control

In the first approach, a threshold is considered for the TEC module to start working. In other words, when the cell temperature exceed a specific limit the TEC module will start working and does not allow the cell temperature to increase anymore. Intuitively, a controller will be needed to adjust the required supplied power to the TEC in each condition (solar radiation, ambient temperature and wind speed). In this approach, the TEC operation acts as a shield for the solar cell which keeps it from degradation due to high cell temperature. Considering solar radiation of 2000 W/m^2, the required electrical power for the TEC module to keep the PV cell temperature lower than 340 K for different ambient temperatures is presented in Table 9. As can be seen, for higher ambient temperature more power will be needed to provide cooling for the PV cell.

Table 9: Required power to keep PV module temperature under 340 K in different ambient temperature for solar radiation of 2000 W/m^2

T_{amb}	I_c	P_{TEC}	P_{Net}
300	0	0	2.9
301	0.24	0.0451	2.8838
302	0.25	0.046	2.8515
303	0.3	0.1229	2.7655
304	0.39	0.3422	2.5577
305	0.45	0.4853	2.4033
306	0.54	0.8357	2.0605
307	0.6	1.0439	1.8389
308	0.69	1.5234	1.363
309	0.8	2.0881	0.7995
310	0.88	2.7372	0.1492

Also for a constant ambient temperature of 300 K, the required power to keep the PV cell temperature under 340 K for different solar radiation levels is presented in Table 10. It is obvious that for higher solar radiations more power is required to keep the cell at the desired temperature.

Table 10: Required power to keep PV module temperature under 340 K under different solar radiation for ambient temperature of 300 K

G	I_c	P_{TEC}	P_{Net}
2000	0	0	2.97
2100	0.25	0.0324	3.0287
2200	0.45	0.4372	2.8155
2300	0.55	0.7516	2.64
2400	0.75	1.64	1.93
2500	0.95	2.86	0.8775

The results show that the PV-TEC system is capable of keeping the cell temperature under a specified limit for different conditions by using the generated power via PV cell itself. PV modules usually utilized along with a battery to save the generated energy when it is more than required. This energy can be utilized later to keep the cell cool and avoid any potential damages. Intuitively, considering the meteorological conditions in a specific area during the

year, the PV module itself and the required power, an appropriate TEC module needs to be selected with a controller for adjusting the supplied power.

Output Power Enhancement

Another approach can be defined to use PV-TEC system when the goal is enhancing the net output power from the combined PV-TEC system by adjusting the supplied current to the TEC module. Increasing the electrical current would increase the cooling effect which in turn leads to less cell temperature and higher output power. However, on the other hand, more electrical current means more power consumption by the TEC module. There is a trade-off between the extra generated power due to cell temperature reduction and TEC power consumption. Therefore, the objective function is defined as the power saving due to temperature reduction in the PV module minus the utilized power by the TEC module. The optimization variable is the electrical current which feeds the TEC module. Therefore, for a fixed considered ambient temperature and solar radiation, the GA finds the optimal value of I_c which yields the highest output power.

The considered objective function is calculated as below:

$$Extra\ Power = (P_{PV,\ with\ TEC\ cooling} - P_{PV,\ without\ cooling}) - P_{TEC} \qquad (57)$$

where the first term in equation above is the extra generated power due to temperature reduction and the second term refers to the consumed power by the TEC module.

The results from optimization of the system are given in Table 11. It should be noted that the performance of the system is strongly dependent on the Z value (figure of merit) of the thermoelectric module which is considered to be 0.007 for this simulation which is higher than typical available TEC modules available in market. As can be seen, the optimal value for the

electrical current has a small magnitude. It can be seen that for this case, it is possible to generate extra power due to cooling effect of the TEC module via the PV panel. This extra power is more than the utilized power by the TEC module for the optimal value of the I_c. However, for the optimal I_c the cooling effect is not very significant and the temperature reduction did not exceed 8 K.

Table 11: Optimal values of I_c for maximizing net output power

G (W/m^2)	T_{cell} (K) Without cooling	T_{cell} (K) With cooling	I_{opt} (A)	Extra Power (W)	Net Output Power (W)
1500	340.15	335.8	0.4	0.0062	2.0643
2000	350.45	344.71	0.5	0.055	2.6
2500	360.49	353.41	0.61	0.116	3.029
3000	370.29	361.9	0.7	0.1866	3.35

Obviously, for a TEC module with a small value of Z value, and a PV module with lower power temperature coefficient, there might be no optimal point. In other words, if the generated power by the PV would be less affected by the cell temperature increment, few degrees reduction in cell temperature cannot generate more power than the utilized power for the TEC module. This is shown in Table 12 where the ambient temperature is set at 311 K and the solar radiation is considered to be 2000 W/m^2, the extra generated power due to temperature reduction for TEC modules with different values of Z is presented. It can be seen that for Z value less than 0.005 there will be no extra generated power by using PV-TEC system which is the scenario for most of the current available modules in market.

Table 12: The magnitude of extra generated power for different values of *Z*

Z (1/K)	T_{cell} (K) Without cooling	T_{cell} (K) With cooling	I_{opt} (A)	Extra Power (W)	Net Output Power (W)
0.005	350.45	345.32	0.46	0.004	2.55
0.006	350.45	345.01	0.48	0.036	2.58
0.007	350.45	344.71	0.5	0.055	2.6
0.008	350.45	344.41	0.52	0.0704	2.62

As can be seen, using TEC modules can provide fair amount of cooling for the PV cell which results in generating extra amount of power. The extra power increases at higher radiation levels

In practice, since the solar radiation, as well as ambient temperature is varying during the time, an active control system is required to keep the current at an optimal level. The control system needs to adjust the value of electrical current based on the solar radiation and/or cell temperature.

The purpose of this latter study was to evaluate the use of Peltier effect for cooling PV cells. As it can be seen, although using TEC modules can provide rather good cooling effect for the PV cell, it uses significant amount of power which is a drawback for this application in comparison with commonly used active cooling methods. All active cooling approaches need some extra power e.g. pumping power or fan power for PVT-water and PVT-air systems. The advantage of using TEC cooling over air/water cooling systems can be listed as below:

- No need for pumping and plumbing
- The cooling system is supplied by the PV cell itself
- More appropriate for small applications

- Accurate controllability
- Light and quiet

CHAPTER 5: CONCLUSION

In this research, three main thrusts are considered and investigated by computer simulation via MATLAB:

- A photovoltaic-thermal collector system which used air flow for cooling is modeled and investigated under different solar radiation levels. The model is then used to evaluate the performance of the system in Tuscaloosa, AL. the effect of tracking, concentration and cooling is investigated and the annual performance is calculated and depicted via several graphs for each case.

- The combined use of photovoltaic cell and thermoelectric power generator modules (PV-TEG) is modeled and analyzed. Three simulations were carried out to investigate the performance of a single PV-TEG system, a solar panel with 36 TEG modules under different solar radiation levels and finally the daily and the annual performance of a combined PV-TEG system in weather condition for Tuscaloosa, AL. The result shows using TEG can add up to 3.95 % to the generated power by a PV cell when the radiation is 2600 W/m^2. A sensitivity analysis is also carried out to study the effect of thermal resistance and ambient temperature on the performance of the system.

- The performance of a combined photovoltaic-thermoelectric cooling (TEC) system has been evaluated. For this purpose, an analysis is conducted on combined PV-TEC systems in order to evaluate the performance of the cooling effect provided by TEC modules on PV cells to, *a)* control the temperature for specific applications, and *b)* enhance the total output power due to temperature reduction. The result shows that

the combined PV-TEC system can be used for both approaches, but have limited applications with current TEC modules in the market.

The results show that there is a fairly good potential of using concentrating photovoltaic systems in south east US. A Siemens SP 75 solar panel is considered for simulation and the result shows that the simple PV panel can generate about 82 kWh/yr electricity and the system which benefits from single axis tracking, 2X concentration and an air cooling channel can generates 177 kWh/yr which seems promising.

Although the analysis shows that combined PV-TEG systems under low level concentrations can produce considerable extra power, further investigation on thermoelectric materials and high concentration level CPVs might be able to achieve higher output power. The combined PV-TEC systems where the TEC module is used to control the temperature looks promising for small applications where PVT's cannot be used. The use of TEC modules to enhance the net power generated by the system can also be promising for some specific applications specially for higher figure of merits and when the voltage temperature coefficient of the cell is rather high and the power loss due to temperature increment is very significant.

FUTURE WORKS

- Validation of the results of computer simulation via experimental work
- Performance evaluation of the systems under medium and high level concentration
- Performance analysis of the PVT system in Alabama area using other cooling fluids (e.g water, refrigerant)
- Second law analysis of the systems
- Designing a controller for the PV-TEC system which can keep the PV cell temperature at the appropriate level.
- Economic analysis of the PVT, PV-TEG and PV-TEC systems.
- Investigating the thermoelectric modules at the pellet level (rather than module level).

REFERENCES

[1] *National Solar Radiation Data Base: TMY3.* http://rredc.nrel.gov/solar/old_data/nsrdb/1991-2005/tmy3/. Web. 1 Jun 2012.

[2] Data compiled by Lawrence Kazmerski. *Best Research Cell Efficiencies National Renewable Energy Laboratory*, National Center for Photovoltaics. http://www.nrel.gov/. Web. 05 March 2012.

[3] Parida, B, Iniyanb, S, and Goic, R, "A review of solar photovoltaic technologies", *Renewable and Sustainable Energy Reviews* 15 (2011) 1625–1636.

[4] Mousazadeh, H, Keyhani, A, Javadi, A, Mobli, A, Abrinia, K, and Sharifi, A. "A review of principle and sun-tracking methods for maximizing solar systems output", Renewable *and Sustainable Energy Reviews* 13 (2009) 1800–1818.

[5] Garboushian, V, Roubideaux, D, and Yoon, S. "Integrated high-concentration PV near-term alternative for low-cost large-scale solar electric power." *Solar Energy Mater Solar Cells* (1997);47(1–4):315–23.

[6] Verlinden, PJ, Terao, A, Daroczi, S, Crane, RA, Mulligan, WP, and Cudzinovic, MJ. "One-year comparison of a concentrator module with silicon point-contact solar cell to a fixed flat plate module in Northern California." In: *Proceedings of the 16th European photovoltaic solar energy conference*, May 1–5, (2000), Glasgow, UK, 2000.

[7] Koronakis, PS. "On the choice of the tilt angle for south-facing solar collectors in the Athens basin." *Solar Energy* (1986);36:217e25.

[8] Zahedi, A. "Review of modelling details in relation to low-concentration solar concentrating photovoltaic." *Renewable and Sustainable Energy Reviews* 15 (2011) 1609–1614.

[9] Viana, T.S, Ru¨ther, R, Martins, F.R, and Pereira E.B, "Assessing the potential of concentrating solar photovoltaic generation in Brazil with satellite-derived direct normal irradiation." *Solar Energy* 85 (2011) 486–495.

[10] Gómez-Gil, FJ, Wang, X, and Barnett, A. "Energy production of photovoltaic systems: Fixed, tracking, and concentrating." *Renewable and Sustainable Energy Reviews* 16 (2012) 306–313.

[11] Mallick, TK, Eames, PC, Hyde, TJ, and Norton, B. "The design and experimental characterization of an asymmetric compound parabolic photovoltaic concentrator designed for building integration in the UK." *International Journal of Ambient Energy*, (2004) 25 (2). pp. 85-96.

[12] Matsushima, T, Setaka, T, and Muroyama, S. "Concentrating solar module with horizontal reflectors." *Solar Energy Materials & Solar Cells* (2003);75:603–12.

[13] Huang, BJ, and Sun, FS. "Feasibility study of one axis three positions tracking solar PV with low concentration ratio reflector." *Energy Conversion and Management* (2007);48:1273–80.

[14] *Harnessing the sun through concentratio*n. http://opelinc.com/news/opel-solar-inc-and-betasol-secure-spanish-feed-in-tariff-for-one-of-worlds-first-commercial-hcpv-power installations/. Web. 01 Jun 2012

[15] Edenburn, M.W. "Active and passive cooling for concentrating photovoltaic arrays." *Conference record, 14th IEEE PVSC*, (1980), pp. 776–776.

[16] Araki, K, Uozumi, H, and Yamaguchi, M. "A simple passive cooling structure and its heat analysis for 500x concentrator PV module", *Conference record, 29th IEEE PVSC*, (2002), pp. 1568–1571.

[17] Feldman, K.T, Kenney, D.D, and Edenburn, M.W, "A passive heat pipe cooled photovoltaic receiver." *Conference record, 15th IEEE PVSC*, (1981), pp. 165–172.

[18] Florschuetz, L.W, Truman, C.R, and Metzger, D.E. "Stream wise flow and heat transfer distributions for jet array impingement with crossflow." *J. Heat Transfer* 103 (1981) 337 342.

[19] O'Leary, M.J, and Clements, L.D. "Thermal-electric performance analysis for actively cooled, concentrating photovoltaic systems." *Sol. Energy* 25 (1980) 401–406.

[20] Royne, A, Dey, C.J, Mills, D.R. "Cooling of photovoltaic cells under concentrated illumination: a critical review", *Solar Energy Mater. Solar Cells* 86 (2005) 451e483.

[21] Chow, T.T, "A review on photovoltaic/thermal hybrid solar technology." *Applied Energy* 87 (2010) 365–379.

[22] Hongxia, Xia, Lingai, Luob, and Gilles, Fraisse, "Development and applications of solar-based thermoelectric technologies", *Renewable and Sustainable Energy Reviews,* 11 (2007) 923–936.

[23]*High-power Thermoelectric Cooling Module*. http://www.sinocool.com/chanp/ ShowArticle. asp?ArticleID=44. Web. 01 Jun 2012.

[24] *Power generator makes electricity from heat* http://www2.electronicproducts.com/ Power_generator_makes_electricity_from_heat-article-pspo02_apr2009-html.aspx. Web. 1 Jun 2012.

[25] *Thermoelectric Cooler*. http://www.razorconcepts.net/ thermoelectrics.html. Web. 01 Jun 2012.

[26] Rockendorf, G, Sillmann, R, Podlowski, L, and Litzenburger, B. "PV-hybrid and thermoelectric collectors." *Solar Energy* (1999);67:227–37.

[27] Vorobiev, Y, González-Hernández, J, Vorobiev, P, and Bulat, L." Thermal-photovoltaic solar hybrid system for efficienct solar energy conversion." *Solar Energy* 2006;80:170–6.

[28] Tritt, TM, Böttner, H, and Chen, L. "Thermoelectrics: direct solar thermal energy conversion." *MRS Bull* (2008);33:366–8.

[29] Muhtaroglu, A, Yokochi, A, and Von Jouanne, A. "Integration of thermoelectrics and photovoltaics as auxiliary power sources in mobile computing applications." *J Power Sources* (2008);177:239–46.

[30] van Sark, W.G.J.H.M. "Feasibility of photovoltaic-Thermoelectric hybrid modules." *Applied Energy* 88 (2011) 2785–2790.

[31] *Strong PV Demand*. http://www.renewableenergyworld.com /rea/news/article/2010/08/ strong-pv-demand-in-2009-2010-and-2011. Web. 01 Jun 2012.

[32] *Introduction to Photovoltaic Systems*, SECO FACT SHEET NO. 11.

[33] http://www.samlexsolar.com/learning-center/solar-cell-module-array.aspx

[34] *Photovoltaic Research*, http://www.nrel.gov/pv/. Web. 0.1 Jun 2012.

[35] *Concentrating Photovoltaics*,http://www.greenrhinoenergy.com/solar/technologies/pv_concentration.php. Web. 09 Feb 2012.

[36] *Fresnel Lens*. http://en.wikipedia.org/wiki/Fresnel_lens. Web. 01 Jun 2012.

[37] Skoplaki, E, and Palyvos, JA. "Operating temperature of photovoltaic modules: a survey of pertinent correlations." *Renew Energy* (2009);34:23–9.

[38] Skoplaki, E, and Palyvos, JA. "On the temperature dependence of photovoltaic module electrical performance: A review of efficiency/power correlations." *Sol Energy* (2009);83:614–24.

[39] Chow, T.T, "A review on photovoltaic/thermal hybrid solar technology." *Applied Energy* 87 (2010) 365–379.

[40] Sarhaddi, F, Farahat, S, Ajam, H, and Behzadmehr, A, "Exergetic performance assessment of a solar photovoltaic thermal (PV/T) air collector." *Energy and Buildings* 42 (2010) 2184–2199.

[41] Wong, L.T, and Chow, W.K, "Solar radiation model." *Applied Energy* 69 (2001) 191–224.

[42] Incropera, Frank. P, and DeWitt, David P. *Fundamentals of heat and mass transfer*. John Wiley, 2007. Print.

[43] Saloux, E, Teyssedou, A, and Sorin, M, "Explicit model of photovoltaic panels to determine voltages and currents at the maximum power point." *Solar Energy* 85 (2011) 713–722.

[44] Wilcox, S, and Marion, W, "Users Manual for TMY3 Data Sets", *National Renewable Energy Laboratory*, 2008.

[45] Li, Z, Liu, X, and Tang, R, "Optical performance of inclined south-north single-axis tracked solar panels." *Energy* 35 (2010) 2511e2516.

[46] Koronakis, PS. "On the choice of the tilt angle for south-facing solar collectors in the Athens basin." *Solar Energy* (1986);36:217e25.

[47]Lave, Matthew, and Kleissl, Jan. "Optimum fixed orientations and benefits of tracking for capturing solar radiation in the continental United States." Renewable Energy 36 (2011) 1145e1152.

[48] Joshi, A.S, Tiwari, A, Tiwari, G.N, Dincer, I, and Reddy, B.V. "Performance evaluation of a hybrid photovoltaic thermal (PV/T) (glass-to-glass) system." *International Journal of Thermal Sciences* 48 (2009) 154–164

[49] *Solar Tracking Application*, www.rockwellautomation.com.Web. 01 Jun 2012.

[50] Huang, B.J, and Sun, F.S. "Feasibility study of one axis three positions tracking solar PV with low concentration ratio reflector." *Energy Conversion and Management* 48 (2007) 1273–1280.

[51] *Thermoelectric Cooling Modules Application Note*, MAGALAND TECHNOLOGY, INC. http://www.magaland.com/TECAN.pdf. Web. 11 May 2012.

[52] Zhang, H.Y. "A general approach in evaluating and optimizing thermoelectric coolers." *international journal of refrigeration* 33(2010)1187e1196.

[53] Holland, J. *Adaptation in Natural and Artificial System*, University of Michigan Press, Ann Arbor, 1975. Print.

[54] Goldberg, D.E. *Genetic Algorithms in Search, Optimization, and Machine Learning*. Addison-Wesley Longman, Inc., 2000. Print.

[55] Konak, A, Coit, D, and Smith, A. "Multi-objective optimization using genetic algorithm: A tutorial", *Reliability Engineering and System Safety* 91 (2006) 992–1007.